








## Article

# Unraveling Soundscape Dynamics: The Interaction Between Vegetation Structure and Acoustic Patterns

Giorgia Guagliumi <sup>\*</sup>, Claudia Canedoli , Andrea Potenza , Valentina Zaffaroni-Caorsi , Roberto Benocci , Emilio Padoa-Schioppa  and Giovanni Zambon 

Department of Earth and Environmental Sciences (DISAT), University of Milano-Bicocca, Piazza Della Scienza 1, 20126 Milano, Italy

\* Correspondence: g.guagliumi@campus.unimib.it

**Abstract:** Ecoacoustics examines the interactions between soundscapes, ecological processes, and anthropogenic disturbance. Acoustic communication is crucial for wildlife, making noise pollution a key factor in shaping biodiversity, though its effects are also modulated by habitat characteristics. In this work, we assess the influence of highway noise and vegetation structure on the soundscape and avian distribution of the Moriano oxbow lake (Beregardo, PV, Italy), a Site of Community Importance in the Ticino Valley Regional Park. A two-week monitoring campaign (April 2022) used eight recorders arranged in a grid to analyze soundscape dynamics through eight ecoacoustic indices (ACI, ADI, AEI, BI, NDSI, H, DSC, ZCR). Vegetation surveys quantified tree diversity and structural parameters such as basal area, height, stem density, biomass, and leaf cover. Correlation analyses revealed that *Quercus robur* abundance and tree diversity significantly influenced the acoustic environment, while bird richness correlated positively with vegetation biomass and *Quercus robur* presence. Highway proximity was a key structuring factor, with indices (ADI, H, NDSI, ACI) increasing with distance. These findings underscore the dual role of noise and vegetation in shaping soundscapes and highlight the importance of incorporating habitat features into ecoacoustic assessments to better understand biodiversity patterns in anthropized landscapes.



Academic Editor: Siu-Kit Lau

Received: 31 March 2025

Revised: 24 April 2025

Accepted: 29 April 2025

Published: 6 May 2025

**Citation:** Guagliumi, G.; Canedoli, C.; Potenza, A.; Zaffaroni-Caorsi, V.; Benocci, R.; Padoa-Schioppa, E.; Zambon, G. Unraveling Soundscape Dynamics: The Interaction Between Vegetation Structure and Acoustic Patterns. *Sustainability* **2025**, *17*, 4204. <https://doi.org/10.3390/su17094204>

**Copyright:** © 2025 by the authors. Licensee MDPI, Basel, Switzerland. This article is an open access article distributed under the terms and conditions of the Creative Commons Attribution (CC BY) license (<https://creativecommons.org/licenses/by/4.0/>).

**Keywords:** ecoacoustics; soundscape; traffic noise; vegetation survey; habitat structure; bird community

## 1. Introduction

Sound is a fundamental yet often overlooked component of ecosystems, shaping the behavior, distribution, and interactions of organisms that produce and perceive it. However, increasing anthropogenic noise is altering natural soundscapes worldwide, posing emerging threats to biodiversity and ecosystem function. Soundscape ecology has therefore emerged as a crucial field to investigate these dynamics, analyzing the interplay between biological, anthropogenic, and geophysical sound sources across spatial and temporal scales [1]. In this context, the concept of soundscapes has become an essential tool to understand how human activities disrupt natural acoustic patterns and interact with biotic and abiotic components of ecosystems, with implications for species communication, habitat selection, and ecosystem resilience. This multidisciplinary approach makes it possible to monitor the health of ecosystems, identify sources of acoustic stress, and assess the impact of sound dynamics on the organism's present [2]. Understanding how vegetation mediates the effects of anthropogenic noise is essential for biodiversity conservation, especially in

fragmented or peri-urban forest ecosystems that are increasingly exposed to human pressures. Birds in particular rely heavily on acoustic communication, and chronic exposure to noise can disrupt mating, territorial defense, and foraging behavior, ultimately leading to shifts in community composition. Identifying how landscape structure can mitigate these effects provides crucial insights for developing more effective management strategies in the face of increasing anthropization.

The soundscape of a place is shaped by a series of factors. For instance, vegetation has a crucial role in modulating the sound environment, influencing not only sound propagation but also the interactions between living organisms [3]. Several studies have shown that vegetation structure, tree cover density, and diversity can significantly model the soundscape of an area, modifying the refraction and absorption of sound waves [4]. The interaction between anthropogenic noise and vegetation structure is crucial in shaping the soundscape. Vegetation not only affects sound propagation but also modulates the impact of noise on biodiversity, particularly for species like birds that depend on acoustic signals for communication. In addition, vegetation should be considered as it plays a crucial role in providing nesting and feeding sites for bird communities; these roles need to be taken into account when assessing the impact of anthropogenic noise on bird communities. Studying soundscape dynamics in anthropized landscapes presents unique challenges due to the overlap of natural and anthropogenic sound sources, the spatial and temporal variability of human activities, and the heterogeneity of land use. These factors make it difficult to isolate biotic acoustic patterns and often obscure the ecological signals of interest. In addition, anthropogenic noise can mask or alter important biological sounds, making it difficult to assess ecosystem health or species abundance using passive acoustic methods. Addressing these issues requires careful study design at an appropriate scale and a robust methodological framework capable of disentangling overlapping signals. However, the relationships between soundscape and vegetation are complex and differ significantly according to the environmental contexts, including the presence of anthropogenic disturbances. Indeed, a better understanding of the anthropogenic component impacts requires local-scale studies to be adequately dimensioned to consider the landscape role. Despite increasing attention to the role of vegetation in shaping the acoustic environment, previous research has largely focused on either sound propagation mechanisms or biodiversity responses, often neglecting the integrated analysis of forest structure and anthropogenic noise. Furthermore, few studies have investigated these dynamics at the local scale, where landscape heterogeneity and human pressures interact in complex ways. This study aims to address this gap by combining ecoacoustic metrics with detailed structural vegetation analysis to investigate how forest characteristics influence soundscape composition and the spatial distribution of avian communities in anthropized forest ecosystems.

To deal with this complexity, the use of ecoacoustic indices has gained popularity in recent years. These quantitative metrics simplify the analysis of the soundscape, focusing on different sound characteristics [5], allowing for the assessment of specific acoustic features and providing a more comprehensive picture of the environment's complexity [6]. In fact, the use of multiple indices allows the acquisition of more specific information regarding different aspects of sound, such as sound pressure, sound quality, and directionality; it enables the adaptation of analyses to specific application needs, such as the assessment of environmental noise or sound quality; and it reduces the likelihood to obtain a non-exhaustive or biased interpretation of the sound environment [7].

The main objective of this study is to investigate how vegetation structure modulates soundscape composition in forested ecosystems exposed to different levels of anthropogenic disturbance, with a particular focus on the spatial distribution of avifauna. By integrating ecoacoustic indices with forest structural variables, this research aims to identify patterns

and potential thresholds in noise–vegetation–fauna interactions. These findings can inform future ecoacoustic assessments by highlighting the importance of considering vegetation attributes when interpreting acoustic data, especially in contexts where human activity is present. Ultimately, the study contributes to the development of more accurate and context-sensitive tools for biodiversity monitoring and conservation planning.

The structure of the paper is organized to reflect the logical flow of the research. Section 2 outlines the study area and the methods used for data collection and analysis. The ecoacoustic survey is described first, including instrumentation, index calculation, and statistical analyses. This is followed by the vegetation assessment, which details the estimation of structural parameters and tree biomass, as well as the analysis of vegetation variables. The final part of the Section examines the correlations between acoustic indices and vegetation metrics. Section 3 presents the main results, while Section 4 discusses the results in the context of the existing literature. Section 5 concludes the paper by summarizing the main findings and implications of the study.

## 2. Materials and Methods

### 2.1. Study Area

The study area is located near the Moriano oxbow lake, within the Ticino Valley Regional Park, near Bereguardo (PV). The Moriano oxbow lake is a meandering wetland formed by the natural evolution of the Ticino River. Although partially isolated from the current river flow, it remains hydrologically and ecologically connected to the surrounding river system. Oxbow lakes such as Moriano are important for the conservation of biodiversity as they provide refuges for aquatic and semi-aquatic species and contribute to the ecological complexity of riverine landscapes. The area is set in the north-western Pavia province, along the left bank of the Ticino River, at the end of the Naviglio canal of Bereguardo (Figure 1a). This region covers a surface area of approximately 39 hectares and includes a significant portion of the floodplain, as well as the Ticino valley depression and the adjacent low plain. The main anthropogenic element influencing the area is the A7 highway (Figure 1a, in red), known as the “Autostrada dei Giovi”, which is one of the principal arterial roads connecting two main urban centers: Milan to Genoa. This infrastructure has a significant impact both acoustically and ecologically, contributing to noise pollution and fragmentation of the natural habitat [8].

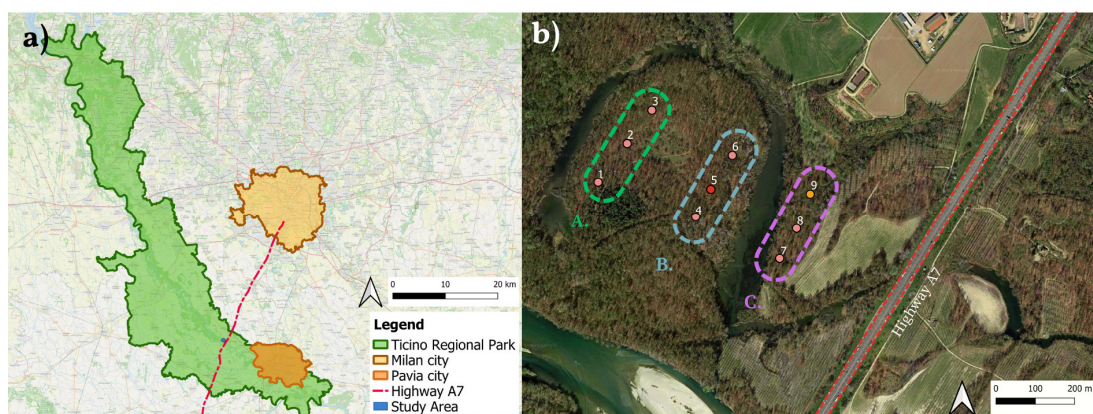


**Figure 1.** (a) Map of the study area at the Moriano oxbow lake in the Ticino Valley Regional Park, Bereguardo, highlighting the A7 highway (in red) as the main source of anthropogenic disturbance. (b) Study area divided into three spatial bands: band A (sites 1, 2, 3) and band B (sites 4, 5, 6) located within the oxbow, and band C (sites 7, 8, 9) positioned nearer the highway. The pink and orange dots represent different recording instruments, while the red dot indicates the instrument lost during the monitoring campaign.

The area is part of the Site of Community Importance (SIC) IT2080014 “Basso Corso e Sponde del Ticino”, designated for its valuable natural habitats and the presence of species of community interest. In particular, the area supports a mosaic of habitats including riparian woodland, gravel bar vegetation, dry grassland, and aquatic and hygrophilous herbaceous communities. These habitat types support a wide range of fauna including amphibians, birds, and invertebrates of conservation concern. The ecological heterogeneity and transitional nature of the oxbow lake environment reinforce its role as a biodiversity hotspot within the Park. These habitats and species are vital for preserving biodiversity at the European scale. Conservation measures focus on protecting these habitats, restoring species populations, and promoting sustainable ecosystem management in accordance with the European Commission’s Habitats Directive (92/43/EEC) [9].

## 2.2. Ecoacoustic Measurement Campaign

Nine measurement sites distributed along a regular grid and covering different habitat types were chosen as the study area, highlighting the importance of environmental heterogeneity [10]. The disposition of the sites was designed to align the measuring instruments parallel to the main source of disturbance, represented by the A7 highway. This spatial subdivision makes it possible to capture both the environmental variability and the gradual transition between the environments closest to the anthropogenic disturbance and those located within the oxbow. To minimize the potential effects of spatial autocorrelation, the sites were selected not based on spatial proximity, but rather to represent a gradient of anthropogenic disturbance and vegetation types. This approach allowed for a more robust analysis of soundscape dynamics while reducing the risk of spatial redundancy and ensuring variability across the sampling points.

The measurement grid comprises three distinct bands (Figure 1b): Band A (sites 1, 2, and 3), situated within the oxbow; Band B (sites 4, 5, and 6), also within the oxbow but farther from the river; and Band C (sites 7, 8, and 9), positioned outside the oxbow near the highway. This configuration allows for a more precise assessment of the impact of anthropogenic noise generated by vehicle traffic on the surrounding ecosystem. The exact coordinates of the sampling sites, recorded in WGS84 format, are provided in Table 1.

**Table 1.** Geographic coordinates and habitat characteristics of the sampling sites in the study area (WGS84 format).

Site ID	Latitude (°N)	Longitude (°E)	Habitat Characteristics
Sito 1	452°371'234	90°229'544	Fragmented patch of exotic bamboo species
Site 2	452°380'494	90°239'421	Mixed broadleaf vegetation, near a clearing
Site 3	452°387'879	90°246'892	Mixed broadleaf vegetation, near a clearing
Site 4	452°363'020	90°261'236	Dense mixed vegetation structure
Site 6	452°377'732	90°273'191	Sparse oak woodland
Site 7	452°353'633	90°288'446	Closest to the oxbow lake
Site 8	452°360'432	90°294'009	Near forestry area
Site 9	452°368'756	90°298'826	Near forestry area

From the acoustic point of view, temporal sampling was structured on long-term monitoring periods, distributed over several seasons. For each season, recordings were made for two consecutive weeks, according to the following scheme: 1 min of continuous recording; 5 min of break.

In the context of this article, the data analyzed derive from the 2022 spring campaign, which took place from April 13th to 27th. Parallel to the acoustic recordings, field surveys were conducted to characterize the forest structure.

### 2.3. Measurement Devices

Nine audio recording devices were used for the study, in particular: eight Song Meter Micro (SMM, measurement sites no. 1–8) by Wildlife Acoustic and a Soundscape Explorer Terrestrial (SET, measurement site no. 9) developed by Luniletronik. Both types of recorders were programmed to operate at a sampling rate of 48 kHz.

SMM recorders have a single microphone with a maximum sampling frequency of 96 kHz. The sensitivity of the entire signal transmission chain (i.e., microphone, amplifier, and analogue-to-digital converter) is  $2 \text{ dBV} \pm 4 \text{ dBV}$  relative to 1 Pa at 1 kHz Full-Scale, measured using a gain of +18 dB. Although this type of device is suitable for long-term recordings in natural environments, it has a non-linear frequency response, which can affect the accuracy of acoustic analyses. During a spectral analysis of the recordings, a Direct Current (DC) offset was found in the SMM devices, with the exception of the device installed at site 6. This problem, which introduces a DC component into the audio signal, can alter the waveform and affect the spectrographic analysis of the signal. In particular, the offset creates a peak in the first frequency bin, distorting the spectral energy distribution and affecting the calculation of ecoacoustic indices. The removal of the DC offset was essential to ensure the correctness of subsequent analyses; this was achieved by calculating the mean value of the audio signal and subtracting the offset from each sample, realigning the waveform around the ideal mean value of zero [11]. This procedure aligns with the mean estimation method, one of the most commonly employed strategies for DC offset correction in periodic-discrete signals [12]. The adoption of this technique guarantees adherence to established IEEE signal processing standards and has been validated for ecoacoustic applications in studies such as Potenza et al. (2023) [11].

The SET device, on the other hand, is a programmable recorder equipped with two microphones with a maximum sampling frequency of 48 kHz and 192 kHz, respectively, and several environmental sensors (capable of measuring parameters such as humidity, temperature, brightness, and atmospheric pressure), having a near-flat frequency response up to 6 kHz. The microphone has a sensitivity of  $-28 \text{ dBV} \pm 3 \text{ dBV}$  relative to 1 Pa at 1 kHz.

As regards the vegetation area, a Canon EOS model M50 MARK II camera equipped with a fisheye lens was used to assess the leaf coverage of the measurement area.

### 2.4. Soundscape Characterization

#### 2.4.1. Calculation of Ecoacoustic Indices

Ecoacoustic indices were used to monitor the soundscapes and quantify acoustic dynamics within the study area. These indices facilitate the distinction between natural and anthropogenic sounds, providing concise and reliable metrics to assess the relationships between the soundscape and the biological and ecological components of the environment [13].

In this study, the calculation of ecoacoustic indices was carried out using the R programming language, through the packages ‘tuneR’, ‘seewave’, and ‘soundecology’, tools specially designed for the analysis of audio data in the scientific domain [14]. The spectral analysis of the signals was performed using the Fast Fourier Transform (FFT), with a window of 1024 points. This provides a spectral resolution of 46.87 Hz, which is considered optimal for obtaining a detailed and accurate analysis of the recorded acoustic components.

Considering the complexity of sound ecosystems, the use of a single ecoacoustic index would be insufficient for an exhaustive understanding of the studied environment. Therefore, a multi-index methodology was adopted in this research, including eight ecoacoustic indices, each capable of capturing different aspects of the soundscape [7]. The indices selected are: the Acoustic Complexity Index (ACI) [15], the Acoustic Diversity Index (ADI) [16], the Acoustic Evenness Index (AEI) [16], the Bioacoustic Index (BI) [17], the

Normalized Difference Soundscape Index (NDSI) [18], the Acoustic Entropy (H) [19], the Dynamic Spectral Centroid (DSC) [15], and the Zero Crossing Rate (ZCR) [20]. We selected these acoustic indices due to their frequent application in recent ecoacoustic studies, across a variety of contexts including general soundscape research [21], natural ecosystems [22], and urban environments [23]. This choice reflects their proven ability to capture complementary dimensions of acoustic complexity, biodiversity, and anthropogenic disturbance in different ecological settings.

The parameters used to calculate them, such as minimum and maximum frequency and sound intensity threshold (dB), were chosen to focus the analysis on the biophonic component of the soundscape [24]. The methodological process involved the selection of a day with suitable meteorological conditions, in which there was no significant precipitation and the wind speed was moderate, to avoid meteorological interference on the recordings. Subsequently, the analysis was divided into three specific time bands: dawn, characterized by increased bird activity; sunset, a period associated with courtship behavior or territorial defense of certain species; and an intermediate time band to compare acoustic variations [25].

To identify the minimum biophonic frequency (corresponding to the maximum frequency of the anthropogenic noise), we examined the spectrograms of the recordings using the frequency visualization property of the Kaleidoscope software. This frequency was determined based on the presence of only anthropogenic noise, thus eliminating all traces of biophony.

The maximum frequency was determined through the identification of the avifaunal species present in the field, using the limited distance point count method [26]. The songs of each species were obtained from the Xeno-Song database [27], and the maximum species-specific frequencies were identified using Audacity [28]. The highest frequency found among the detected species was chosen as the maximum value for the calculation of the ecoacoustic indices.

For the processing of the ADI and AEI indices, the original scripts [29] were modified to include the minimum frequency as a parameter, in line with the approach used for other indices, such as ACI, BI, NDSI, and DSC, which already take this parameter into consideration. This improved the sensitivity of the indices to changes in the soundscape, resulting in a more accurate representation of ecoacoustic dynamics.

The acoustic diversity and uniformity indices also require the inclusion of a sound intensity threshold, i.e., `dB_threshold`, which establishes a minimum decibel level above which sounds are considered relevant for analysis. To define this parameter, the focus was placed on the analysis of the biophonic vocalizations in the recordings, considering even the most distant and weakest ones. Using the same day and time periods, the spectrograms were examined with Kaleidoscope [30], allowing the intensity level of the less prominent vocalizations to be estimated and the “`dB_threshold`” to be established accurately.

Since different types of recorders were used, it was necessary to equalize the recordings to obtain a frequency response comparable to that of a sound level meter. This step resulted in uniform sound levels and ecoacoustic indices derived from the recordings. To achieve this, the recorders' frequency response was compared with the sound level meters, and a corrective filter was subsequently generated to ensure equivalence between the two instruments.

The procedure adopted consists of three main steps: I. the measurement of a white noise using both a sound level meter and the recorders in the field; II. the generation of a filter in the frequency domain, calculated based on the ratio between the Power Spectral Density (PSD) of the recordings made by the sound level meter and the recorders; III. the application of the obtained filter to all the recordings acquired during the measure-

ment campaign. The technical details of this procedure are described in the study [11], where the MATLAB (R2023a) script for implementing the technique is available in the Supplementary Materials.

#### 2.4.2. Statistical Analysis

To identify which ecoacoustic indices perform a predominant role in the characterization of the soundscape of the study area, the Principal Component Analysis (PCA) was applied. This approach reduces the dimensionality of the data, highlighting the variables that better explain the total variance, facilitating the interpretation of the relationships between the indices and the monitored sites [31]. Before performing the PCA, the data were subjected to a scaling pre-treatment using the 'prcomp' function in the R software, setting the option 'scale = TRUE'. This step normalized the data, ensuring that each variable (the ecoacoustic indices) had a mean of zero and a standard deviation of one. Scaling was crucial to prevent indices with different ranges of values from excessively influencing the PCA results, while keeping the information content intact.

The analysis focused on the average values of ecoacoustic indices calculated for each site during the period one hour before and two hours after sunrise, when birdlife is particularly active. Subsequently, graphs were generated in R to visualize which ecoacoustic indices contribute most to the first two principal components (PC1 and PC2). These graphs provide a visual representation of the distribution of the variables and show which indices have the greatest influence in explaining the total variance of the dataset. To visually identify which variables contribute most to each of the principal components, the function "fviz\_contrib" from the "factoextra" package in R was used [32]. This function creates a bar graph representing the contribution of each variable to the selected components. A dashed reference line is drawn on the graph, indicating the expected contribution in the case of a uniform distribution of the variables. Columns above this line represent variables with an above-average contribution, suggesting that they have a particularly strong influence on determining the first dimensions of the PCA. This approach allows us to focus on the most significant ecoacoustic indices to explain the principal components, facilitating a clearer understanding of the sound dynamics of the studied area.

A temporal descriptive analysis was performed on the average values of ecoacoustic indices for each site. Boxplots of the average indices for different time frames (diurnal/nocturnal) were created to refine the analysis and facilitate comparisons between the conditions.

### 2.5. Vegetation Assessment

#### 2.5.1. Data Collection and Vegetation Index Calculation

To analyze the forest structure, field surveys were carried out in 9 plots, each associated with a soundscape recording site. Following standard protocol, starting from the central tree on which the recording instrument was placed, a square area with a side of 30 m was delimited [33]. The delimitation was performed using a measuring wire and a compass to ensure maximum precision. In each plot, data were collected regarding the site, the date of the survey, the operators involved, the habitat type, the percentage of herbaceous and shrub cover, the ground necromass, and the presence of standing dead trees and stumps. For each tree within the plot, the height and circumference of the trunk were recorded using a telemeter to measure the height and a meter to measure the circumference at a height of 1.30 m above the ground.

These measurements allowed the calculation of structural parameters that are fundamental to describe the vegetational structure of the site:

- H (Height): height measured with the telemetric laser.

- DBH (Diameter at Breast Height): diameter of the trunk measured at a standard height of 1.30 m above the ground, derived from the ratio of circumference (C) and pi.
- SD (Stem Density): density of woody biomass per unit area, obtained by dividing the total number of trees by the plot area. The results were converted to trees per hectare (trees/ha) to ensure comparability with literature data.
- BA (Basal Area): cross-sectional area of the trunk measured at 1.30 m from the ground. This parameter provides a volumetric indication of the space occupied by the tree biomass, which is useful to evaluate the structure of the site and predict its evolution. From these parameters, indices describing the structure of the vegetation were calculated:
- RSD (Relative Stem Density): expressed as a percentage, was calculated as the ratio between the density of the species under consideration and the total density of the plot [34].
- RD (Relative Dominance): dominance of a tree species based on its basal area, calculated as the ratio between the basal area of the species under study and the total basal area of the plot.

Lastly, the following biodiversity indices were used to characterize ecological diversity: species richness, proportion of individuals per species, Shannon index, and Evenness.

To optimize the vegetation analysis in the various plots, a pivot table was created to quickly obtain an overview of the tree species present and the values of the vegetation indices for each species. This approach facilitated large-scale data processing, allowing the index values for each plot to be summed up accurately and efficiently. Subsequently, the aggregated data were organized into a comprehensive database, showing the sum of the indices for each species present in the analyzed plots. This provided a clear view of the differences between the areas studied, allowing a direct comparison of vegetation structures and ecological dynamics within the various plots.

### 2.5.2. Tree Biomass Calculation and Allometric Equations

To estimate the epigeal tree biomass and enrich the vegetation database, allometric equations were used in accordance with the 2003 IPCC guidelines [35]. In forestry, allometry refers to the statistical relationships that link the different structural dimensions of trees. Plants belonging to the same population, growing under similar environmental conditions, maintain consistent proportions between more easily measurable parameters (such as diameter and height) and more complex variables (such as volume or biomass). These relationships provide an accurate estimate of biomass from simple measurements by applying allometric equations [36].

The IPCC guidelines recommend the use of species-specific allometric equations or expansion factors to estimate the amount of carbon stored in trees. In the present study, biomass was calculated through allometric relationships based on basic dendrometric parameters such as diameter at breast height (DBH) and tree height (H), where available; where height was not measured, only diameter was used.

The selection of appropriate allometric equations was carried out through the Glob-AllomeTree [37] platform, an international resource developed by FAO, CIRAD, and the University of Tuscia (UNITUS). This platform provides access to a large database of allometric equations, allowing the selection of the most suitable ones for biomass calculation in different geographical areas.

For each tree species identified in the study plots, the most suitable allometric equation was selected, shown in Table 2, following the specific criteria:

- Geographical proximity of the equation to the study area, preferably within the same Country or climatic region.

- Presence of both dendrometric variables (height and diameter) to ensure accurate biomass estimation.
- Details on the components analyzed, such as bark, dead branches, gross branches ( $D > 7$  cm), thin branches ( $D < 7$  cm), leaves, large roots, fine roots, medium roots, stump, trunk-underbark, and fruit/seed.

**Table 2.** Selected allometric equations for each tree species present in the study plots, following the specific criteria explained above.

Tree Species	Allometric Equation
<i>Carpinus betulus</i>	$0.0485 * (DBH)^2 * H + 5.4$
<i>Gleditsia triacanthos</i>	$0.05138 * (DBH)^{2.739} * 1.1117$
<i>Pinus sylvestris</i>	$0.05138 * (DBH)^{2.739} * 1.1117$
<i>Quercus robur</i>	$-1.0906 + 0.031073 * (DBH)^2 * H$
<i>Populus Nigra</i>	$0.0662 * (DBH)^2 * H + 4.9$
<i>Ostrya carpinifolia</i>	$0.0662 * (DBH)^2 * H + 4.9$
<i>Alnus glutinosa</i>	$0.00079 * (DBH)^{2.28546}$
<i>Fraxinus excelsior</i>	$10^{-2.4598 + 2.4882 * LOG(DBH)}$
<i>Populus alba</i>	$0.0662 * (DBH)^2 * H + 4.9$
<i>Prunus padus</i>	$10^{-0.06657 + 1.7041 * LOG(H)}$
<i>Populus canescens</i>	$0.0662 * (DBH)^2 * H + 4.9$
<i>Ulmus minor</i>	$2.04282 * (DBH^2)^{1.25462}$
<i>Robinia pseudoacacia</i>	$4.13741 * (DBH^2)^{1.08876}$

Tree biomass was quantified by applying these equations to trees with a diameter at breast height (DBH) greater than 5 cm.

Subsequently, the biomass values for each species were aggregated, generating an overall biomass value for each plot. This approach provided an overall view of the tree biomass distributed in the various habitats, being useful for subsequent ecological analyses and for understanding the contribution of different species to the structure of the forest landscape.

### 2.5.3. Data Acquisition Using Remote Sensing Techniques

The last two indices analyzed to enrich the vegetation database are the Plant Area Index (PAI) and the Vegetation cover fraction (FCover). The PAI represents the amount of foliage in a plant ecosystem relative to the underlying land area, providing a measure of the density and leaf cover of the vegetation. FCover, on the other hand, indicates the fraction of land area covered by vegetation, proving particularly useful for monitoring changes in vegetation cover over time. In this study, hemispherical photography was used as a proximal sensing technique to estimate these parameters. Although not strictly remote sensing, this ground-based approach provides valuable structural information on canopy characteristics through the analysis of in situ fisheye images.

To estimate these parameters, hemispherical images were acquired using a Canon EOS M50 MARK II camera with a fisheye lens. Five images were taken at each study site: one directly under the tree housing the acoustic recording instrument, and the other four at a distance of five meters, diagonally across the vertices of a square [38].

The images obtained were analyzed using the CAN-EYE software, developed by the Environnement Méditerranéen et Modélisation des Agro-Hydrosystèmes (EMMAH) and the French National Institute of Agronomic Research (INRAE) [39]. CAN-EYE is an advanced canopy structure analysis software that extracts information from the vegetation cover through RGB images acquired with traditional or fisheye lenses.

The analysis phase required an initial pre-processing of the images, during which:

- The photographs were configured as RGB colour hemispheric images, oriented upwards;
- Configuration parameters such as day of the year and latitude (45° N) were entered, as well as camera-specific calibration parameters.

Subsequently, an image classification phase (both automatic and manual) was performed, in which the pixels associated with the sky cover were distinguished from the pixels referring to the vegetation (Figure 2).

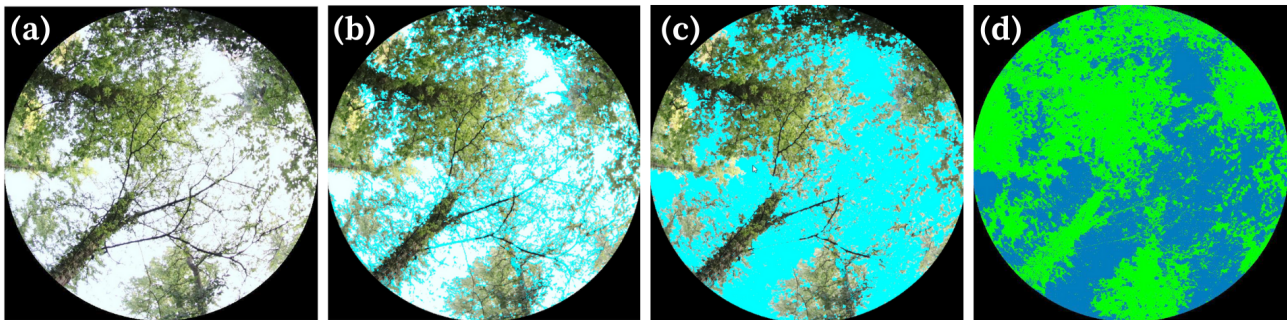


**Figure 2.** Image processing procedure: (a) The original image is imported into the analysis software; (b) automatic classification starts, where the pixels are separated into “sky” (in blue) and “vegetation”; (c) the classification is manually refined, correcting the wrongly classified pixels and converting them back to “sky”; (d) improving the distinction between sky and vegetation, increasing contrast and saturation for better visualization, iterating the previous steps.

#### 2.5.4. Vegetation Variables Analysis

To describe the forest structure in a general way, the surveyed tree species were divided into different diametric classes based on DBH. Nine diametric classes were defined, with intervals of 10 cm each. For each survey plot, the total number of individuals per diametric class and species was counted [40]. These values were subsequently converted to a hectare basis to standardize the data.

For each plot, the following parameters were reported: (1) the number of individuals per diametric class for each species; (2) the total number of individuals per species; and (3) the total number of individuals in the plot (obtained by summing the individuals of all species present). These data permitted the analysis of the specific composition of the community and the assessment of the size structure distribution of the tree population for the different species. The vegetation indices were subjected to a principal component analysis (PCA) to reduce complexity and identify which variables contribute most to explaining the variance in the data. In particular, through the examination of variable loadings for each component, we could determine which vegetation indices were most correlated with the first and second dimensions, providing key insights into the predominant variables in the characterization of vegetation structure. Given the structural interdependence of certain vegetation parameters (e.g., basal area, stem density, biomass and vegetation cover), some degree of multicollinearity is to be expected. However, the application of PCA is particularly appropriate in this context, as it reduces redundancy by transforming correlated variables into orthogonal components, thereby mitigating the potential inflation of variance due to collinearity [41].

To further support the use of PCA as a dimensionality reduction method, we also computed a Spearman correlation matrix among the vegetation variables. This analysis confirmed moderate-to-high correlations between structurally related parameters, as expected in forest ecosystems. The matrix is provided as Supplementary Figure S1.

## 2.6. Soundscape and Vegetation Correlations

To further analyze the data, several specific distances were calculated using QGIS software [42]. Distances between the sampling points and specific ecological and anthropogenic elements of the study area were measured. In particular, the following distances were considered:

- Dist\_A7: Distance from the A7 highway to assess the influence of road noise and landscape fragmentation.
- Dist\_la: Distance from the oxbow edge to examine the effect of water proximity on vegetation and bird species.
- Dist\_ra: Distance from the clearing, an open area within the forest, to investigate its impact on local biodiversity.
- Dist\_fi: Distance from the river, to explore its influence on vegetation composition and biodiversity based on moisture and riparian habitat characteristics.
- Dist\_ba: Distance from a dense bamboo plot, an artificial structure, or a distinctive feature in the study area.
- Dist\_mb: Distance from the forest edge, to understand the ecological gradient between the forest interior and more open areas.

First, a preliminary check of the data distribution was conducted using the Shapiro–Wilk test [43] to assess the normality of the variables. This step was necessary to determine the correct statistical approach to be taken in the next phase. Based on the test results, variables were categorized as normally or non-normally distributed. Pearson’s correlation was used for normal variables, while Spearman’s coefficient was applied for non-normal ones, ensuring robust analysis. These analyses were performed in R, and significance was set at  $p \leq 0.05$ .

Due to the accidental loss of the recording device at Site 5, data from this location were excluded from the analysis, resulting in a total of eight sampling sites. While this number ensures spatial representation of the oxbow and surrounding areas, we acknowledge that the limited sample size reduces statistical power. Consequently, results from statistical tests should be interpreted with caution. Given the small sample size, the Shapiro–Wilk test for normality may not be fully reliable. For this reason, Spearman’s correlation, which is less sensitive to non-normality, was preferred in borderline cases to ensure robustness. This approach is consistent with recommendations in the literature that emphasize the robustness of Spearman’s when normality assumptions are questionable or when sample sizes are too small to support parametric methods [44].

### Correlation Between Arboreal Size and Avian Richness

To assess the relationship between tree size and avian richness, vegetation variables were analyzed, focusing on the ecological role of large trees. These provide nesting sites and food resources for birds, particularly arthropods found in bark, woody tissues, and epiphytic layers on higher branches [45]. The analysis included both primary cavity nesters, such as woodpeckers, which create their own cavities, and secondary cavity nesters, such as titmice and creepers, which utilize existing cavities [46]. Habitat preferences were considered, with primary nesters favoring mature forests and woodpeckers adapting to fragmented landscapes, to account for variations in forest structure and maturity.

In the study area, the dominant tree species, selected based on size and presence across all sampling plots, was identified and considered for further analysis. To obtain an accurate estimation of avian species richness, acoustic data were processed using Raven Pro software [47], which facilitated the identification of bird species through the analysis of vocalizations recorded between dawn and dusk (06:00–18:00). For species identification, a specific day was selected for analysis, corresponding to a public holiday with optimal

meteorological conditions (i.e., absence of strong winds or precipitation) to minimize environmental variability. The species were then classified with the support of the BirdNET library [48], comparing the results with the Ticino Park lists.

Subsequently, the correlation between bird species richness (obtained via BirdNET) and the percentage of individuals of the dominant tree species per diameter class was calculated. Correlation analysis was performed using Spearman's correlation coefficient due to the non-parametric distribution of the data. All statistical analyses were carried out in the R environment, using the stats package [49].

To strengthen the analysis, the same procedure was applied to a younger and more abundant tree species in the study area to test the hypothesis that there was no significant correlation between smaller tree species and bird richness.

### 3. Results

#### 3.1. Soundscape Values Characterization

The results indicate a maximum anthropogenic frequency of 1700 Hz for bands A and B, and 1750 Hz for band C. The value of 1750 Hz was selected as a representative threshold for the entire study area.

Spectral analyses revealed that traffic noise predominantly occupies low-frequency ranges, with negligible variations among spatial bands. The aural inspection of recordings confirmed this pattern, showing a persistent presence of low-frequency noise that can be traced back to the highway.

The maximum biophonic frequency identified was obtained by investigating the frequencies emitted by birds present in the study area. Thus, the frequency range attributable to local avian species was found to be between 1.75 kHz and 9 kHz.

Lastly, regarding the dB threshold, the relative dB values across three different time slots (6:00 a.m., 12:00 p.m., and 7:00 p.m.) were initially averaged to consider the variability of biophony throughout the day. Specifically, the threshold levels were found to be  $-71$  dB for the early morning period (5:00–8:00 a.m.),  $-73$  dB for the midday period (11:00 a.m.–2:00 p.m.), and  $-72$  dB for the evening period (6:00–9:00 p.m.). These values were then averaged, resulting in a final threshold of  $-73$  dB.

##### 3.1.1. Statistical Analysis

A PCA was performed to reduce the dimensionality of clustering variables while preserving the significance of the statistical metrics describing the index distribution. In line with the widest possible variance of the original variables, we selected the first two dimensions because they have a cumulative percentage of explained variance,  $V$ , given by  $V1 + V2 = (68.5 + 17.3)\% = 85.8\%$ . The value  $V \geq 80\%$  is commonly used as a cut-off to decide which principal components to keep [41]. In our case, we use the first two components (or eigenvectors, referred to here as dimensions) of the PCA to reduce the total number of variables.

The contributions of the two dimensions are shown in Figure 3. The red threshold corresponds to the expected mean value of the contribution if all variables contributed uniformly to the variance explained for that dimension. Specifically, this threshold is calculated as  $1/n \times 100\%$ , where  $n$  is the total number of variables considered. The variables with the largest contributions to Dim-1 were found to be H, ZCR, AEI, ADI, and BI (Figure 3a), all with contributions above the significance threshold of 12.5%.

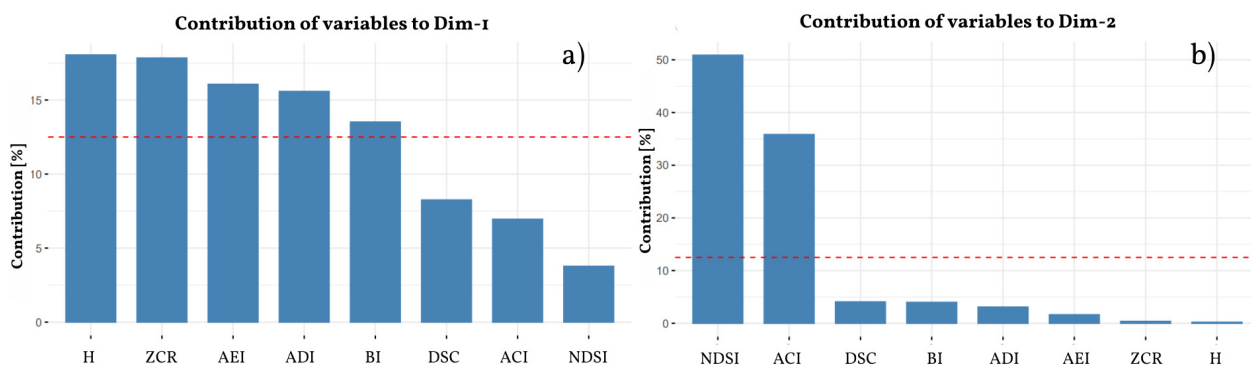


**Figure 3.** Contribution of each ecoacoustic index to the first (a) and second dimensions (b). The dashed lines indicate the value of equal contribution.

### 3.1.2. Temporal Trends of Ecoacoustic Indices

Following the PCA, we examined the variables that contributed mostly to the first two dimensions by producing mean time trends and boxplot graphs. Specifically, the variables H and ZCR were analyzed for the first dimension, and NDSI and ACI for the second dimension. These variables were chosen because they represent the main components of variation within the studied soundscape (Figure 3). Specifically, H and ZCR describe the global structure of the soundscape, with an emphasis on spectral and frequency variation, while NDSI and ACI provide a direct measure of ecoacoustic dynamics, highlighting acoustic complexity and the relationship between biophonic and anthropogenic sounds. This choice allows us to capture both general characteristics and more specific ecological aspects of the soundscape.

Temporal analysis of the H-index shows significant differences between sites in relation to their distance from the highway (Figure 4a). In sites far from the infrastructure (1, 4, and 6), H has higher values during diurnal hours, reflecting a more balanced distribution of sound frequencies and greater biophonic complexity. The peaks recorded in the early morning hours can be attributed to the intense songbird activity. In contrast, at sites closer to the highway (7, 8, and 9), H is reduced, highlighting the prevalence of anthropogenic noise, which is characterized by a less diverse energy distribution. Among these, site 9 exhibits the lowest values, highlighting the dominance of a single-frequency band caused by acoustic pollution from the highway. During the night-time hours, the H-index tends to decrease at all sites, with a more pronounced reduction at sites near the highway: at sites most exposed to vehicular traffic noise, the anthropophilic component becomes predominant, leading to a further reduction in entropy values.

The ZCR index trend (Figure 4c) confirms the role of road traffic as a source of continuous, monotonous sound. In the sites close to the highway, ZCR values are lower, reflecting the lower variability of the sound signal. At sites farther away (1, 4, and 6), ZCR shows significantly higher values, due to the presence of sounds characterized by frequent crossings of the zero time axis, typical of complex bird vocalizations. At night, ZCR tends to decrease at all sites, with occasional increases due to the activity of some nocturnal bird species. Comparison between sites shows that the points closest to the highway (7, 8, and 9) exhibit a shifted downward trend, in line with the influence of vehicular traffic, while generally higher values are observed at distant sites.

The NDSI (Figure 4b) shows a marked dominance of anthropogenic noise at sites near the highway, with values close to  $-1$ , indicating a soundscape dominated almost entirely by human activity. At the farther sites (1, 4, and 6), significant daily variations are observed, with higher values during the day due to the presence of the biophonic component. In contrast, at sites 7 and 8, the NDSI increase during the day is limited. Despite its proximity

to the highway, site 9 exhibits higher values, indicating a partial balance between biophonic and anthropogenic contributions.

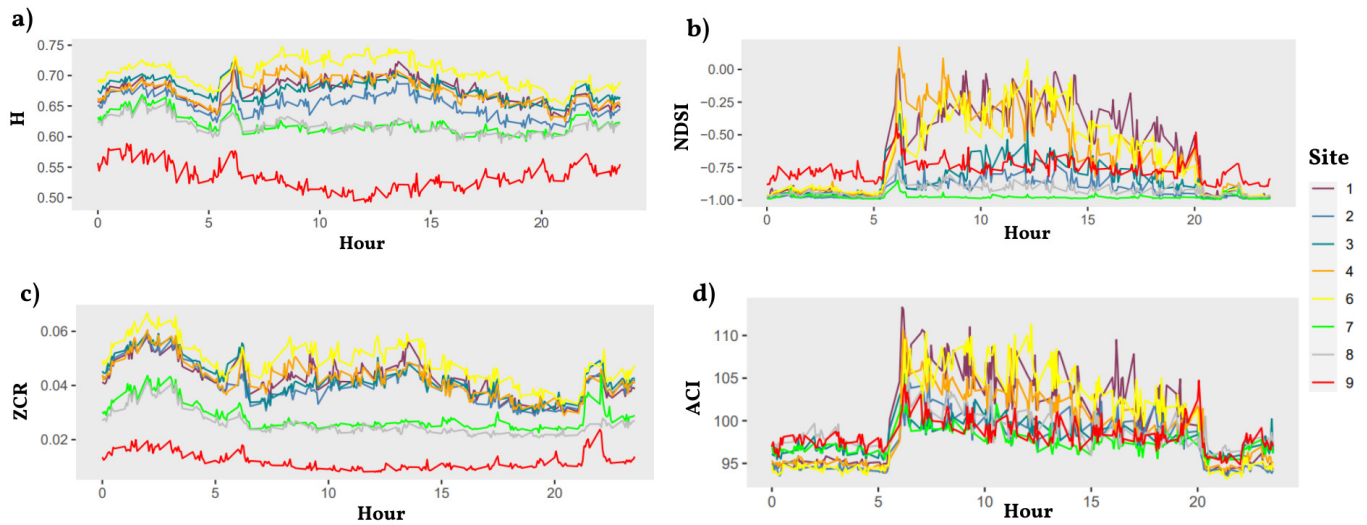


**Figure 4.** Time trends of H (a), NDSI (b), ZCR (c), and ACI (d) averaged by hour for each day and site.

Lastly, ACI (Figure 4d) shows a trend consistent with daytime biophonic activity, which is particularly evident at sites farther from the highway. ACI values peak during the day, especially in the morning, coinciding with bird song activity and other biophonic sounds. At night, ACI decreases dramatically, reflecting reduced biological activity and the prevalence of anthropogenic or stable sounds, such as traffic. At sites 1 and 4, ACI reaches particularly high values, indicative of greater species richness, whereas at sites closer to the highway, values remain lower, reflecting the influence of road noise on the acoustic environment.

The mean hourly boxplots of the ecoacoustic indices (H, ZCR, NDSI, and ACI) show trends consistent with the temporal analyses, highlighting the differences between sites and time slots (Figure 5). The H index reveals a clear distinction between sites close to the highway and those farther away (Figure 5a). Sites 1, 4, and 6 exhibit higher medians with wider interquartile ranges, indicating greater frequency variability and a broader acoustic diversity. Conversely, at sites near the highway (7, 8, and 9), H values are significantly lower, with a more concentrated distribution and fewer outliers. This trend reflects reduced frequency variability, which is characteristic of environments dominated by anthropogenic noise.

Regarding the ZCR index (Figure 5b), the boxplots show greater variability at sites farther from the highway, with higher medians and a wider data distribution. At sites exposed to traffic noise (7, 8, and 9), the medians are lower, indicating reduced acoustic complexity associated with continuous road noise. The diurnal time bands exhibit greater variability than the nocturnal ones, consistent with increased acoustic activity during the day, as observed in the temporal data.

NDSI displays a strongly negative distribution at sites near the highway (Figure 5c), with very low medians (close to  $-1$ ), indicating a soundscape predominantly shaped by anthropophony. At sites 1, 4, and 6, the boxplots show greater variability and slightly more positive values, especially during daylight hours, indicating a stronger presence of biophonic signals. However, even at these sites, the values remain negative on average, reflecting a persistent influence of human-generated noise.

Finally, the ACI boxplot reveals a clear distinction between diurnal sites near and far from the highway (Figure 5d). Sites 1, 4, and 6 have higher ACI values with a wider interquartile range during the daytime hours, reflecting greater acoustic diversity and

wider frequency occupancy. In contrast, at sites closer to traffic (7, 8, and 9), boxplots show lower median values with a narrower distribution, indicating reduced frequency occupancy by biophonic signals. Additionally, ACI values increase during daylight hours, particularly at dawn, when bird song activity is at its peak.

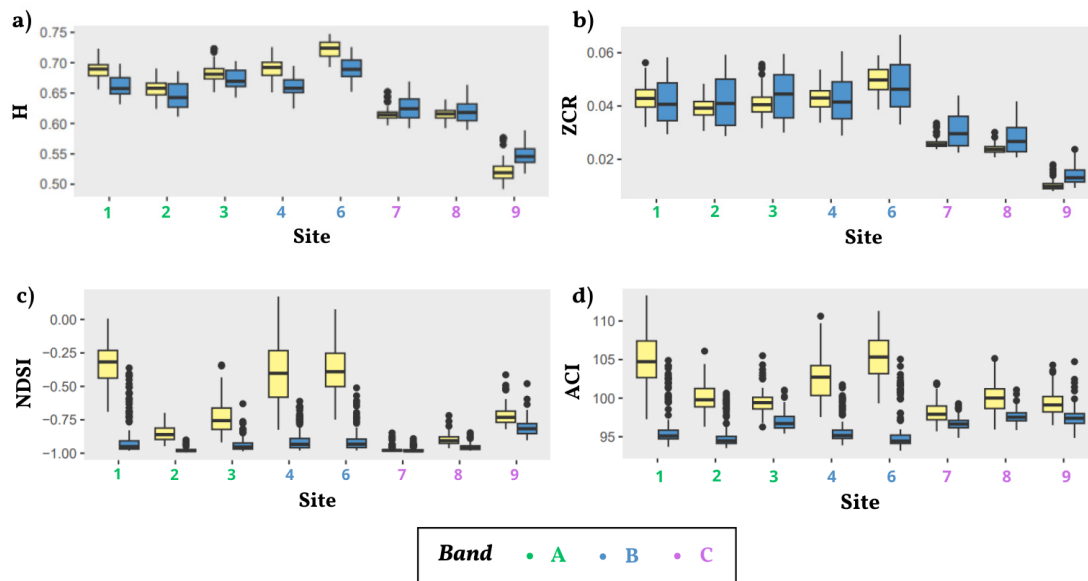


**Figure 5.** Boxplots relating to the trend of the day (in yellow) and night (in blue) phase for each site of the indices: (a) H; (b) ZCR; (c) NDSI; (d) ACI.

### 3.2. Vegetation Assessment

#### 3.2.1. Vegetation Parameters and Forest Structure

The aggregate analysis of the data shows a clear predominance of certain tree species in terms of basal area and relative density. In particular, in plots P1 and P4, *Quercus robur* showed a significantly higher presence than other species, indicating the presence of large mature individuals. The dominant species determined by BA and DBH include *Carpinus betulus*, *Quercus robur*, *Populus nigra*, and *Ulmus minor*, with variations in their distribution between plots (Table 3). In particular, *Quercus robur* recorded the highest BA values in plots P2 and P5 with 814.90 cm<sup>2</sup> and 839.10 cm<sup>2</sup>, respectively. HS, which assesses overall biodiversity, ranged from 0.194 to 2.022 across the plots: plot P7 showed the highest HS value (2.02), indicating a more even distribution of species and potentially richer acoustic diversity. In contrast, plots P6 and P8 had lower HS values (0.15 and 1.12, respectively), reflecting less diverse plant communities, which influence the complexity and richness of the local soundscape.

**Table 3.** Forest and biodiversity indices. The values of the variables were summed for each species in each plot.

Plot	BA [tree/ha]	SD [ha]	SR	HS
1	19.61	433.3	39	1.49
2	8.67	244.4	22	1.18
3	26.97	300	27	0.22
4	44.06	288.9	26	2.15
6	20.83	233.3	21	0.96
7	14.87	577.8	52	2.02
8	1.64	611.1	55	1.12
9	43.05	1666.7	150	1.25

SD varies considerably between plots, with the lowest value recorded in P6 (233.3 trees/ha) and the highest in P9 (1666.6 trees/ha). Plot P9, with the largest number of individuals, shows a higher density of broadleaf species, which contribute significantly to the overall biomass of the area. The BA shows similarly marked variations, with the highest values in P9 (43.1 m<sup>2</sup>/ha) and the lowest in P8 (1.6 m<sup>2</sup>/ha). These data indicate that plot P9 hosts larger trees than the other sites, confirming the importance of this site for the conservation of large tree specimens. The Shannon index varies from a minimum of 0.23 in P3 to a maximum of 2.02 in P7, highlighting significant differences in species distribution and composition. In particular, the high biodiversity in P7 is indicative of a well-structured mixed deciduous habitat. On the other hand, the evenness of species distribution, represented by the evenness index E, is lower in P3 and P6, indicating the presence of a lower number of species in these areas (Table 3).

Forest structure was analyzed based on the distribution of tree species within diameter classes. The graphs (Figure 6) show the number of individuals per species in each plot (P1–P9), highlighting different vegetation configurations and forest structure and maturity. The Table S1 in the Supplementary Materials show the percentage of individuals per species by diameter class.

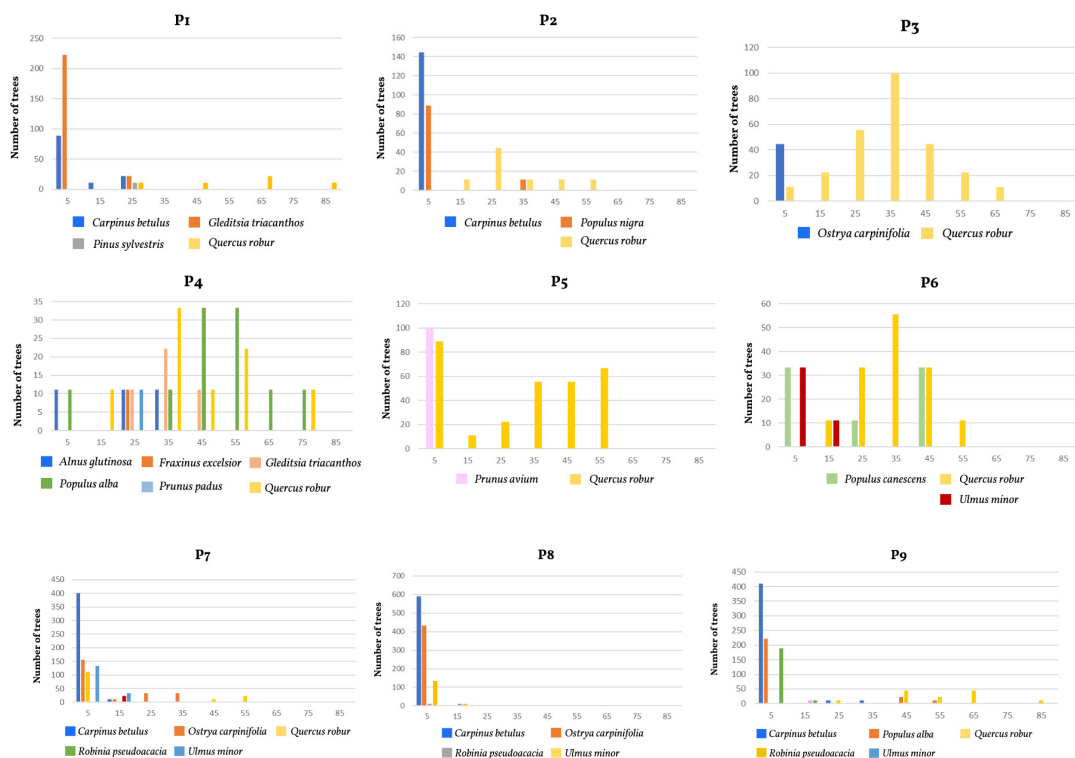


**Figure 6.** Number of individuals per species in the different plots (P1–P9), divided by diameter classes (x-axis).

### 3.2.2. Aboveground Tree Biomass and Vegetation Cover Fraction

The allometric equations, calculated for each individual in each plot according to the equations given in Table 2, were used to estimate tree biomass. The biomass values for each species were then aggregated to give a unique biomass value for each plot. These results, presented in Table 4, showed a difference in the distribution of biomass between the plots.

To quantify the vegetation cover and the amount of foliage in the different plots, the Plant Area Index and Fcover were calculated. The results, presented in Table 4, show differences in the cover fraction between the plots. In particular, plot P7 has the highest Fcover value, indicating a higher vegetation density than the other plots analyzed. This

result highlights a greater vitality and robustness of the plant community in P7, which has a direct impact on the acoustic biodiversity and ecological integrity of the area.

**Table 4.** Aboveground Tree Biomass, PAI, and Fcover Indices for the Different Plots.

Plot	Biomass [kg]	PAI	Fcover
1	15,621.26	2.21	0.45
2	6977.25	2.46	0.41
3	23,791.90	2.71	0.7
4	57,477.57	1.74	0.78
6	56,465	1.44	0.54
7	23,968.29	2.51	0.84
8	4316.78	2.3	0.83
9	45,877.20	2.71	0.7

### 3.2.3. Principal Component Analysis

The decision to include only the relative dominance of *Quercus robur* among the species considered is justified by the fact that this species is present in all plots and is the one with the largest size. Furthermore, *Quercus robur* is ecologically important as it is the native species that characterizes the oak and hornbeam planiferous forests of this region. Therefore, RD\_qr provides a robust measure of the relative dominance of the most representative tree species in the context of the observed vegetation, avoiding distortions arising from the presence of less mature or sporadic species.

The first three dimensions together explain 81.3% of the total variance: the first dimension (Dim1) explains 31.7%, the second (Dim2) 28.8%, and the third 20.8%. The analysis of the contributions of the variables to the different dimensions showed that in the first dimension (Dim1, Figure 7a), the variables that contribute most are Evenness, with a contribution of more than 20%, followed by Biomass, Shannon index, and PAI. On the other hand, BA and RD\_qr show lower contributions, while Species Richness (SR) has a negligible contribution. Regarding the second dimension (Dim2, Figure 7b), tree height was the most significant variable, followed by the Relative Dominance of *Quercus robur* and Biomass.

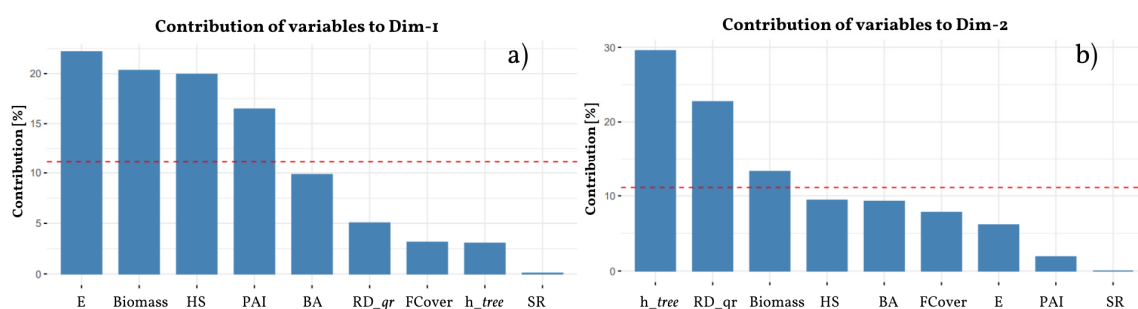


**Figure 7.** Contribution of each original ecoacoustic index to the first two dimensions. The dashed lines indicate the value of equal contribution.

The loading plot (Figure 8) provides a visual representation of the relationships between the variables and the principal components. Along the horizontal axis (PC1), the variables HS and E show a negative correlation with PC1 as they are positioned in the second quadrant of the plot. To a lesser extent, PAI shows a positive correlation with PC1. Along the vertical axis (PC2), the variables Biomass, h\_tree, and RD\_qr are negatively correlated with PC2, as indicated by their position in the third quadrant. Finally, BA and Fcover show respectively negative (third quadrant) and positive (second quadrant) correlations with PC2. These patterns highlight the inverse relationships between certain variables, such as PAI and BA, which are oppositely positioned in the principal component space.

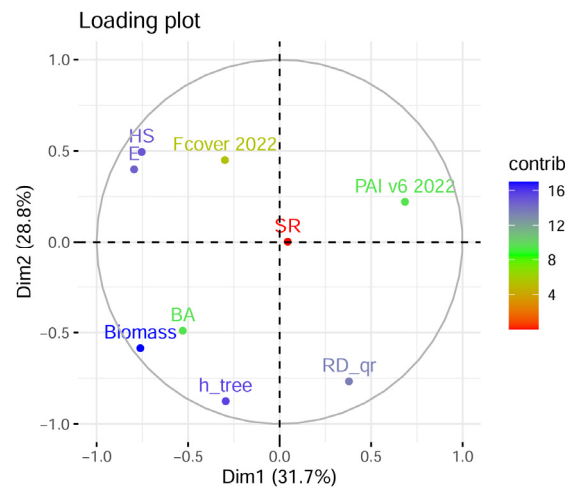


**Figure 8.** Loading plot showing the contribution of the variables to the first two main components.

### 3.3. Soundscape and Vegetation Correlations

The values of the specific distances, shown in Table 5, allow a detailed analysis of the measurements made for each monitoring point. These values were correlated with the ecoacoustic indices and vegetation variables. The analysis revealed statistically significant relationships ( $p$ -value  $\leq 0.05$ ), which are presented in Table 6, together with the calculation methods used.

**Table 5.** Results of specific distances measured for each sampling point. Distances include Dist\_A7 (distance to highway), Dist\_la (distance to oxbow edge), Dist\_ra (distance to clearing), Dist\_fi (distance to river), Dist\_ba (distance to bamboo area, and Dist\_mb (distance to forest edge).

Site	Dist_A7 [m]	Dist_la [m]	Dist_fi [m]	Dist_ra [m]	Dist_ba [m]	Dist_mb [m]
1	774.3	80.1	373.8	92.9	35.5	396.1
2	759.8	96.9	496.7	0	117.2	69.4
3	752.1	93.8	601.6	30.9	212.9	364.8
4	513.7	105	374.4	125.5	134.9	262.2
6	519.4	77.2	560.5	98.3	255.8	172.1
7	275.1	41.6	385.5	330.9	269.2	41
8	278.4	62	468.7	315.3	239.2	52.9
9	298.9	73.5	564.4	311.6	423.6	44.7

**Table 6.** Statistically significant correlations ( $p$ -value  $\leq 0.05$ ) between the variables studied. The third column presents the types of correlations: A for acoustic indices, V for vegetation parameters, and D for specific distances.

Variable 1	Variable 2	Type of Correlation	Correlation	$p$ -Value	Method
NDSI	QUE	A-V	0.73	0.04	Pearson
DSC	RD_qr	A-V	0.76	0.03	Pearson
DSC	Fcover	A-V	-0.79	0.02	Pearson
BI	SR	A-V	0.76	0.03	Spearman
H	Dist_ra	A-D	-0.73	0.04	Pearson
DSC	Dist_A7	A-D	0.81	0.01	Pearson
DSC	Dist_ra	A-D	-0.89	0.01	Pearson
ZCR	Dist_ra	A-D	-0.81	0.02	Pearson
ZCR	Dist_ba	A-D	-0.78	0.04	Pearson
ZCR	Dist_mb	A-D	0.72	0.01	Pearson
HS	Dist_fi	V-D	-0.87	0.01	Pearson
E	Dist_fi	V-D	-0.85	0.01	Pearson
Fcover	Dist_ra	V-D	0.72	0.04	Pearson
Fcover	Dist_mb	V-D	-0.75	0.03	Pearson
Fcover	Dist_A7	V-D	-0.75	0.03	Pearson

The most significant correlations were divided into main groups, focusing on the variables that showed significance in the principal component analysis (PCA). Pearson's correlation coefficient ( $r$ ) was used for linear relationships and Spearman's rank correlation ( $\rho$ ) for non-linear relationships. The most significant correlations were divided into main groups, focusing on the variables that showed significance in the principal component analysis (PCA). These results highlight the relationships between ecoacoustic and vegetation parameters in the different habitats studied.

### I. Correlations between ecoacoustic indices and vegetation variables

The NDSI shows a significant positive correlation with the weighted mean number of *Quercus robur* in the highest diameter classes ( $r = 0.726$ ,  $p = 0.041$ ). Additionally, BI is positively correlated with vegetation species richness ( $r = 0.762$ ,  $p = 0.028$ ). Conversely, DSC exhibits a significant negative correlation with vegetation cover ( $r = -0.793$ ,  $p = 0.018$ ), and is also positively correlated with the relative dominance of *Quercus robur* ( $r = 0.755$ ,  $p = 0.030$ ).

### II. Correlations between ecoacoustic indices and specific distances

The ecoacoustic indices that contribute most to the explanation of the first principal component (PC1) show strong correlations with the distance from the surrounding landscape elements. In particular, ZCR shows a significant positive correlation with the distance from the bamboo scrub (Dist\_ba,  $r = 0.718$ ,  $p = 0.045$ ) and a negative correlation with the forest edge (Dist\_mb,  $r = -0.779$ ,  $p = 0.023$ ). Moreover, both ZCR and H display significant negative correlations with the distance from the clearing (Dist\_ra), respectively ( $r = -0.813$ ,  $p = 0.014$ ) and ( $r = -0.731$ ,  $p = 0.039$ ). Even if DSC does not contribute the most to the PC1, it correlates significantly with the distance from the highway (dist\_A7,  $r = 0.81$ ,  $p = 0.01$ ) and from the clearing (Dist\_ra,  $r = -0.89$ ,  $p = 0.003$ ).

### III. Correlations between vegetation indices and specific distances

The vegetation variables show significant correlations with the distances to the main reference points (Figure 9). In particular, both HS and E, which are important contributors to the PC1, show significant negative correlations with distance to the river (Dist\_fi), respectively ( $r = -0.867$ ,  $p < 0.01$ ) and ( $r = -0.852$ ,  $p < 0.01$ ) (Figure 9).

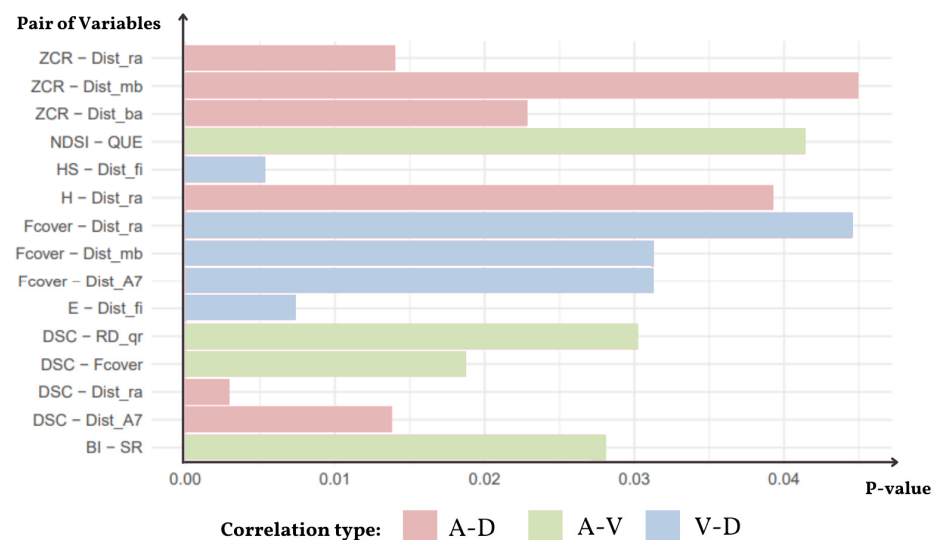


**Figure 9.** Display of statistically significant correlations ( $p$ -value  $\leq 0.05$ ) between the variables studied. The horizontal histograms show the  $p$ -value of the correlations on the  $x$ -axis and the analyzed variable pairs on the ordinates. The colors indicate the three groups of correlations: A for acoustic indices, V for vegetation parameters, and D for specific distances.

### Correlation Between Tree Maturity and Avian Abundance

The data show that *Quercus robur* is the only tree species characterized by larger individuals, observed in all plots except Site 8. Most individuals of this species are found in the higher diameter classes, ranging from class 45 to 85 (40 < DBH < 90 cm). The percentage distribution of *Quercus robur* across diameter classes is shown in the histogram in Figure 10, highlighting a greater concentration of large trees in plots P1, P4, P6, and P9.

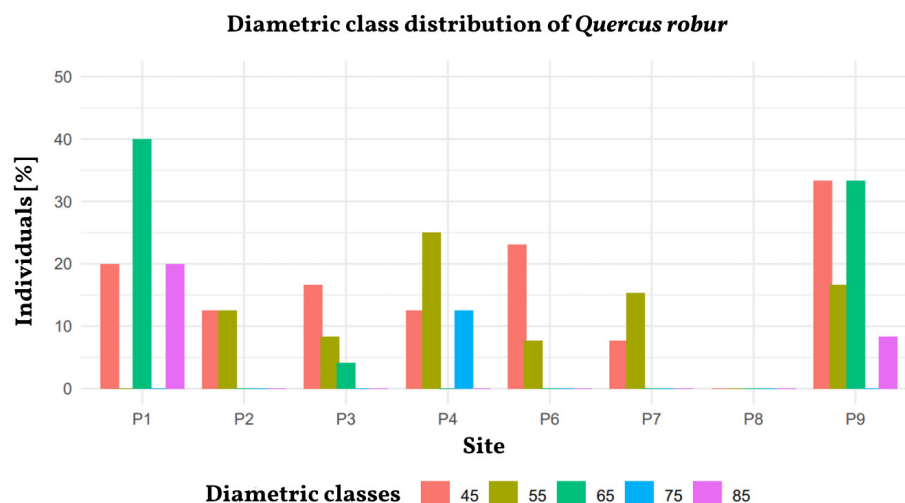


**Figure 10.** Percentage distribution of *Quercus robur* individuals by diameter class in the different plots. The histogram only shows the highest diametral classes, between 40 and 90 cm, highlighting the presence of mature trees.

The results from the Raven analysis reveal significant variation in avian richness between sites (Figure 11). Specifically, sites P1, P6, and P9 exhibit a higher number of species, including both primary and secondary cavity nesters. Furthermore, the presence of avian indicator species, such as *Poecile palustris* and *Certhia brachydactyla*, at sites marked with orange columns (P4 and P6) suggests a relationship between tree maturity and habitat suitability for forest-specialist birds.

We subsequently analyzed the correlation between bird richness and the average number of *Quercus robur* individuals weighted by diameter classes, obtaining a Spearman's coefficient ( $\rho = 0.73$ ,  $p = 0.039$ ), indicating a statistically significant relationship between the variables analyzed. In plots 1, 4, 6, and 9, which are characterized by a higher proportion of *Quercus robur* individuals with a diameter greater than 45 (DBH > 40 cm), a higher bird diversity was observed, especially between primary and secondary cavity nesters. The relationship between tree size and bird diversity is further confirmed by Figure 12, which shows a clear positive relationship between these two variables. The regression line shows that plots with a higher concentration of mature trees tend to support a greater diversity of species, highlighting the crucial ecological role of large trees in the conservation of bird species.

In contrast, *Carpinus betulus*, which is characterized by smaller individuals, shows a predominant distribution in the lower diametric classes. After calculating the weighted average of the percentages of tree individuals in the different diametric classes, the correlation analysis showed a coefficient  $\rho = 0.5$  ( $p = 0.07$ ), confirming the absence of a significant correlation with bird richness. These results confirm the key role of mature tree species in promoting greater biodiversity, while younger individuals, such as those of *Carpinus betulus*, appear to have minimal influence on the presence of bird species.

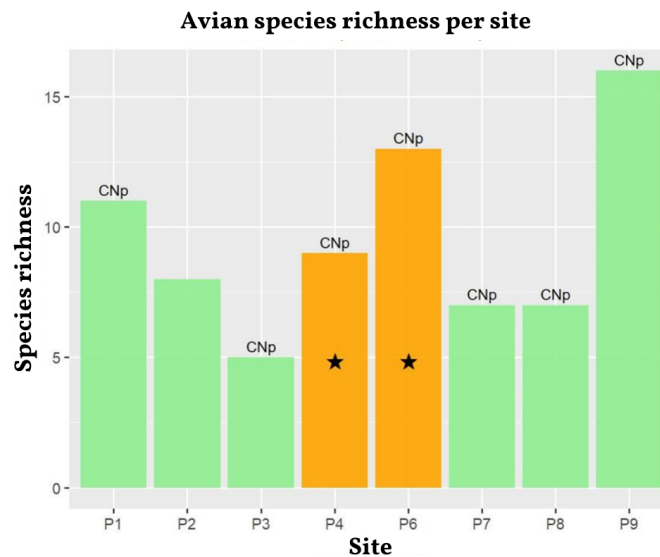


**Figure 11.** Avian richness by site. The histogram shows the total number of avian species for each plot, with specific indications for primary cavity nesters (CNp), positioned above the columns corresponding to the sites where they were found, and for secondary cavity nesters, represented by the symbol ★. The orange columns highlight the sites (P4 and P6) where diversity indicator species, such as *Poecile palustris* and *Certhia brachydactyla*, are present, supporting the link between tree structure and avian biodiversity.



**Figure 12.** Scatter plot with regression line: avian species richness as a function of the percentage of *Quercus robur*.

#### 4. Discussion

The present study addresses the complex interactions between soundscape and vegetation structure in a protected area impacted by anthropogenic noise through a multidisciplinary methodology. Analyzing both the ecoacoustic indices and vegetation structure allowed for a detailed characterization of the spatial and temporal variability of the oxbow's soundscape, highlighting how the proximity to the highway and the vegetation distribution significantly influence the acoustic environment. These results underscore the importance of vegetation as a key element in the attenuation and modulation of anthropogenic noise, and highlight the need for multidisciplinary approaches to enhance the understanding of soundscape patterns.

The methodology used in this study improves the discrimination of acoustic components and emphasizes the need to optimize the employed ecoacoustic indices' parameters to ensure comparability of data across different studies [11,24]. The inclusion of a plurality

of indices [50,51] allowed a more detailed view of the structure of the soundscape, enabling accurate discrimination between biophonic and anthropophonic components. This approach was guided by the evidence reported in the literature, which emphasizes the importance of using specific frequency bands to monitor distinct taxonomic groups. In particular, Metcalf et al. [52] highlight this necessity in their recent publications, limiting their use to a narrower set of indices, such as ACI and BI. Other works, such as the one published by Bradfer-Lawrence et al. [53], also emphasize the aforementioned necessity, albeit to a lesser extent than the other recommendations made in the study. Despite these recommendations, a significant portion of the scientific community continues to use default parameters for the calculation of acoustic indices, while others do not specify the criteria behind the selected values [21,22], or these values are not reported at all [54,55].

Although spatial autocorrelation represents a potential problem in ecological acoustics studies, our sampling scheme aimed to minimize its impact by selecting sites along environmental and anthropogenic gradients, ensuring heterogeneity in vegetation structure and exposure to noise sources. Furthermore, the same recording campaign was analyzed by Benocci et al. (2025) [56], where we applied the Transfer Entropy Measure to the dataset to investigate directional dependencies in the flow of acoustic information. Our results confirmed the presence of spatial differentiation among sites and supported the hypothesis of non-redundancy in the composition of the soundscape. Finally, the authors conducted a direct listening analysis of the recordings [56], which highlighted perceptible differences in acoustic content even between adjacent sites. These insights strengthen the ecological validity of our spatial arrangement, while acknowledging the lack of formal tests of spatial autocorrelation as a limitation to be addressed in future studies.

The trends observed in the ecoacoustic indices (H, ZCR, NDSI, and ACI) analysis clearly reveal a spatial gradient in relation to distance from the motorway. The H-index showed a clear reduction at the sites closest to the noise source, showing a lower sound diversity. In contrast, at more distant sites, H recorded higher values, signaling greater acoustic complexity, due to a richer presence of avian species. Similarly, the mean value of ZCR at sites closer to the highway was significantly lower, reflecting the presence of stable and unvarying acoustic signals, typical of continuous anthropogenic noise [57]. Contrarily, at sites further away, ZCR showed greater variability, associated with the complexity of bird vocalizations. Finally, the NDSI and ACI indices revealed how the balance between biophonic and anthropophonic components varies considerably along the distance gradient. At the sites closest to the highway, the NDSI recorded extremely negative values, suggesting an almost complete dominance of the anthropophonic component [58]. However, in some areas, such as site 9, the NDSI showed slightly higher values than the other neighboring sites, suggesting the presence of some degree of biophony, despite the anthropogenic influence. These results are corroborated by the ACI values, which confirm greater biophonic activity in the early morning hours, particularly at sites further away from traffic [59]. Similarly to our results, the study carried out by M. G. Khanaposhtani et al. [60] in a floodplain forest in Wisconsin (USA)—an ecosystem comparable to the Lanca del Moriano—exposed to the impact of two major highways, reported a significant inverse correlation between ADI, NDSI, and AOI (Acoustic Occupancy Index) with the distance from the road infrastructure. In addition, the inverse gradient between H with highway distance observed at the Lanca del Moriano is in line with the studies carried out at the Parco Nord of Milano, an urban Park also impacted by a highway [61]. These trends can all be explained by the masking effect of traffic that shapes the distribution of local biophony, according to the Acoustic Habitat Hypothesis [62] and other studies. Indeed, López-Bao et al. (2017) confirm that road noise has a significant impact on wildlife, as it masks natural sounds and interferes with the acoustic communication of animals [63]. These effects are

also exposed by other in situ studies worldwide, such as [60], and noise effects on birds are well documented in the literature [64].

Regarding highway noise in ecoacoustics studies, in [60] is highlighted a potential bias in the application of NDSI in environments where noise attenuation occurs due to geometric divergence [60]. This phenomenon has already been documented by R. Benocci et al. in a semi-natural area characterized by herbaceous layers of nemoral flora and a shrub layer, typical of Parco Nord in Milan [61], and by R. B. Machado et al. in a Category V protected area as defined by the International Union for Conservation of Nature (IUCN) [65]. However, the accuracy of the NDSI was improved by the methodological optimization of the input parameters for the calculation of ecoacoustic indices [24], as proposed in the present study. Similarly, cluster analysis further supported the existence of two distinct acoustic configurations, indicating a clear dichotomy between sites dominated by a soundscape rich in biophonic signals and those predominantly influenced by anthropogenic noise. The geometric divergence bias in NDSI could also be present in other indices that present a lower frequency limit (i.e., ADI in [60]), which has been bypassed in this study and in [60] by adding it. On this matter, there is a need to adjust the ecoacoustic indices in the R package “soundecology” to add this parameter, which is already adjusted in the Python library “scikit-maad” [66].

The results regarding vegetation structure and composition reveal a complex landscape, characterized by significant differences between the analyzed plots. These differences are particularly evident when comparing the forest structure and biomass of the sites inside the oxbow (P1–P6) to those near the motorway (P7–P9). This variation in vegetation likely influences the bird community, as differences in habitat complexity and resource availability can impact avian diversity and behavior [67], ultimately shaping the observed sound dynamics [59]. Biomass is significantly higher at sites 4, 6, and 9, indicating a denser vegetation structure and, potentially, richer biophonic activity in these areas [68]. Despite its high biomass, site 9 is located near the highway and shows extremely negative NDSI values, indicating a predominance of the anthropophonic component over the biophonic one. These observations suggest that the masking effect of road noise reduces the ecological benefits of dense vegetation, thereby negatively affecting faunal diversity and activity. This is further supported by the reduced H-index observed at this site, highlighting the negative impact of anthropogenic noise on the complexity of the soundscape [60].

The Shannon index showed high values at sites 4, 1, and 2, indicating greater plant diversity. Interestingly, site 7, located close to the highway, also recorded a high HS value, which can be attributed to the presence of young trees of numerous plant species. However, despite this phase of active habitat renewal, the site-specific ecoacoustic indices suggest that anthropogenic noise associated with the highway influences the soundscape, as indicated by the reduced values of H and ZCR.

The distribution graphs of the diametric classes in the areas closest to the motorway exhibit decreasing curvilinear trends, indicative of an uneven-aged forest structure. This pattern may reflect forest management practices, such as the introduction of new species, which could explain the observed variability in forest composition and structure [69]. At the same time, the scarcity of larger individuals in the sites closest to the motorway indicates a low capacity to support high avian diversity, creating a sub-optimal environment for forest-dwelling species. This result is consistent with that reported by López-Bao et al. (2017), who discussed the negative impact of road networks on biodiversity, including birds, highlighting how road infrastructure can fragment habitats and reduce ecological resources for wildlife [70].

Correlation analysis revealed significant relationships between vegetation structure and ecoacoustic indices. In particular, NDSI showed a positive correlation with *Quercus*

*robur* abundance (QUE,  $r = 0.726$ ,  $p = 0.041$ ), which may indicate that mature trees contribute a stronger biophonic signal to the acoustic environment. This could be related to their structural complexity and ability to support a more diverse faunal community, particularly birds and insects. Previous studies have highlighted how vegetation structure can influence the balance between biophony and anthropophony in soundscapes [13]. However, further research is needed to isolate the specific effect of tree composition from other potential confounding variables such as landscape configuration or proximity to noise sources [19]. Similarly, BI was positively correlated with tree species richness (SR,  $r = 0.761$ ,  $p = 0.028$ ), reinforcing the idea that diverse plant assemblages favor complex acoustic environments by providing diverse habitats and resources for fauna. In contrast, DSC was negatively correlated with FCover ( $r = -0.793$ ,  $p = 0.018$ ), suggesting that denser vegetation attenuates high-frequency sounds, reducing sound propagation and contributing to a more stable acoustic environment.

Significant relationships were also found between the ecoacoustic indices and the spatial distribution of the sampling points. In particular, DSC showed a strong positive correlation with distance from the motorway (Dist\_A7,  $r = 0.814$ ,  $p = 0.013$ ), confirming that increasing distance from traffic sources leads to a reduction in high-frequency noise levels due to sound absorption by vegetation. In contrast, DSC showed a negative correlation with distance from clearing (Dist\_ra,  $r = -0.891$ ,  $p = 0.002$ ), suggesting that open areas characterized by lower vegetation density allow greater sound propagation and higher acoustic energy at high frequencies. Similarly, ZCR, an index of acoustic signal complexity, was negatively correlated with both distance from the bamboo patch (Dist\_mb,  $r = -0.717$ ,  $p = 0.049$ ) and clearing (Dist\_ra,  $r = -0.813$ ,  $p = 0.014$ ). This pattern may reflect higher acoustic variability in transitional or edge environments, which often host a mix of vocal species from both open and closed habitats [19]. However, since ZCR is sensitive to a broad range of high-frequency and transient signals, further investigation is needed to clarify the ecological drivers underlying these values.

Vegetation variables also showed significant correlations with specific distances from sites. In particular, vegetation cover (FCover) was positively correlated with distance from the clearing (Dist\_ra,  $r = 0.718$ ,  $p = 0.044$ ), confirming that moving away from open areas leads to higher forest density. In contrast, FCover was negatively correlated with both distance from the highway and forest edge, suggesting that human disturbance limits vegetation expansion. Furthermore, HS and E are negatively correlated with distance from the river, highlighting the influence of water availability on vegetation structure.

While this study focused on local-scale distances from specific landscape features (e.g., highway, clearing, river), it is important to recognize that broader landscape structure [71], including habitat connectivity and fragmentation across the Ticino Valley Regional Park, likely plays an additional role in shaping avian assemblages. Fragmented landscapes can limit dispersal, reduce nesting site availability, and isolate populations, while well-connected habitats facilitate movement and support higher biodiversity [72,73]. Future research integrating landscape metrics (e.g., patch size, edge density, connectivity indices) derived from remote sensing or GIS analysis could further clarify how large-scale spatial configuration modulates local soundscape and biodiversity patterns.

The positive correlation between NDSI and biomass suggests that vegetation structure plays a fundamental role in shaping acoustic diversity. Forested environments with higher biomass, characterized by well-developed vegetation layers, appear to promote a richer and more complex biophonic component, likely due to their ability to support a greater abundance and diversity of soniferous species [59,60]. This finding is consistent with ecological theories linking habitat complexity to acoustic variability, as structurally rich ecosystems provide enhanced niches and resources for bioacoustic activity [22,26,74].

Furthermore, the observed positive correlation between biomass and bird species richness reinforces the idea that productivity and structural characteristics of vegetation influence the diversity and abundance of bird communities. High biomass levels typically correspond to increased availability of resources, including food sources such as insects and seeds, and nesting sites, which are critical for the persistence of specialized bird species. In particular, mature forest stands dominated by large trees, such as *Quercus robur*, contribute significantly to avian biodiversity by providing microhabitats that support a diverse assemblage of species [67]. The structural complexity of these trees, including their extensive canopies and the presence of cavities, provides essential ecological resources for cavity-nesting birds, a group that is highly dependent on the availability of mature forest elements [75,76].

In addition to their role as physical habitat providers, mature trees may also influence the spatial organization of acoustic signals within forest ecosystems. The hypothesis of acoustic habitat filtering suggests that certain structural features of the habitat may favor species whose vocalizations are best transmitted or least masked in that particular acoustic environment [77,78]. In this context, large individuals of *Quercus robur*, with their complex tree architecture—such as irregular branch angles, cavities, and layered foliage—may generate multiple sound reflections, absorptions, and diffusions. Such structural complexity may lead to the formation of distinct spectral and spatial acoustic niches, facilitating acoustic niche partitioning and enabling the coexistence of bird species that use different frequency bands and calling strategies [79,80]. Our results support this framework, suggesting that the ecological value of mature oak extends to shaping the acoustic landscape in a way that supports diverse acoustic communities.

Conversely, *Carpinus betulus*, although a common tree species at some sampling sites, did not show a significant correlation with avian species richness. This result suggests that tree maturity, rather than mere presence, is a key determinant of avian diversity. Unlike *Quercus robur*, *Carpinus betulus* lacks the structural characteristics necessary to support specialized forest birds, particularly those that rely on cavities for nesting or require stable, resource-rich environments [81]. Its lower ecological contribution may be attributed to its comparatively limited ability to provide trophic and structural resources, reinforcing the idea that forest stands dominated by older, larger trees are critical for maintaining complex and ecologically functional bird communities.

## 5. Conclusions

In this study, we applied a multidisciplinary approach to investigate the interaction between soundscape characteristics and vegetation structure within a protected area affected by a nearby highway. Using eight ecoacoustic indices, we quantified the diversity and complexity of soundscapes at eight sites, revealing a clear distinction between areas exposed to anthropogenic noise and those immersed in denser vegetation. Sites with higher biomass and structurally complex forests, such as sites 4 and 9, showed high acoustic diversity indices, suggesting that mature forests not only provide critical habitat for diverse faunal assemblages but also buffer the propagation of anthropogenic noise. In contrast, areas characterized by simpler vegetation structures and lower biomass, such as sites 2 and 8, were associated with reduced biophony, highlighting the role of habitat quality in shaping acoustic biodiversity.

These results highlight the ability of vegetation to modulate the soundscape by influencing both noise propagation and ecological niche availability. Key structural attributes, such as basal area, tree species richness, and biomass, emerged as primary drivers of ecoacoustic variability, reinforcing the idea that the size of individuals of different habitats plays a fundamental role in supporting biodiversity. In particular, the presence of

large tree species, such as *Quercus robur*, was positively associated with avian species richness, supporting the hypothesis that structural complexity and individual size are critical determinants of both habitat quality and acoustic complexity.

From a broader perspective, this study highlights the value of ecoacoustics as a non-invasive and scalable tool to assess biodiversity patterns and the ecological impact of human activities. Integrating soundscape analysis with vegetation structure assessments provides a powerful framework for understanding ecosystem dynamics, offering new insights into the interactions between biotic and abiotic factors. This approach has significant potential to guide conservation planning, inform sustainable forest management, and mitigate the effects of environmental degradation. Future research should extend these findings by incorporating long-term monitoring strategies, assessing seasonal variations in ecoacoustics models, and exploring the applicability of these methods in different ecological contexts.

By advancing our understanding of how vegetation modulates the soundscape, this study contributes to a growing body of research that supports the conservation of mature forests as a key strategy for maintaining acoustic biodiversity. In an era of rapid environmental change, promoting interdisciplinary approaches that connect ecoacoustics, forest ecology, and conservation science will be essential to safeguard the integrity and resilience of natural ecosystems.

**Supplementary Materials:** The following supporting information can be downloaded at: <https://www.mdpi.com/article/10.3390/su17094204/s1>, Table S1: Percentage of individuals per species by diameter class. Figure S1: Spearman correlation matrix among vegetation variables.

**Author Contributions:** Conceptualization, G.G., A.P., C.C., R.B. and G.Z.; methodology, G.G., C.C., A.P. and R.B.; software, G.G., A.P. and V.Z.-C.; validation, C.C., R.B. and G.Z.; formal analysis, G.G., A.P., V.Z.-C. and R.B.; investigation, G.G., A.P., C.C. and V.Z.-C.; resources, G.Z.; data curation, G.G.; writing—original draft preparation, G.G.; writing—review and editing, C.C., V.Z.-C., A.P. and G.Z.; visualization, G.G. and A.P.; supervision, G.Z. and E.P.-S.; project administration, G.Z.; funding acquisition, G.Z. All authors have read and agreed to the published version of the manuscript.

**Funding:** This research received no external funding.

**Institutional Review Board Statement:** Not applicable.

**Informed Consent Statement:** Not applicable.

**Data Availability Statement:** Data available upon request.

**Conflicts of Interest:** The authors declare no conflicts of interest.

## Abbreviations

The following abbreviations are used in this manuscript:

ACI	Acoustic Complexity Index
ADI	Acoustic Diversity Index
AEI	Acoustic Evenness Index
BI	Bioacoustic Index
NDSI	Normalized Difference Soundscape Index
H	Acoustic Entropy
DSC	Dynamic Spectral Centroid
ZCR	Zero Crossing Rate
H	Height
DBH	Diameter at Breast Height
SD	Stem Density
BA	Basal Area
RSD	Relative Stem Density

RD	Relative Dominance
PAI	Plant Area Index
FCover	Vegetation Cover Fraction

## References

- Pijanowski, B.C.; Farina, A.; Gage, S.H.; Dumyahn, M.A.; Krause, B.L. What is soundscape ecology? *Front. Ecol. Environ.* **2011**, *9*, 203–211.
- Farina, A. *Soundscape Ecology: Principles, Patterns, Methods and Applications*; Springer: Berlin/Heidelberg, Germany, 2014; pp. 1–250.
- Dumyahn, S.L.; Pijanowski, B.C. Soundscape conservation. *Landsc. Ecol.* **2011**, *26*, 1327–1344. [[CrossRef](#)]
- De Coensel, B.; Botteldooren, D.; De Muer, T. Effects of vegetation on the perception of noise in urban parks. *J. Acoust. Soc. Am.* **2011**, *131*, 2731–2739.
- Benocci, R.; Brambilla, G.; Bisceglie, A.; Zambon, G. Eco-acoustic indices to evaluate soundscape degradation due to human intrusion. *Sustainability* **2020**, *12*, 10455. [[CrossRef](#)]
- Depraetere, M.; Pavoine, S.; Jiguet, F.; Gasc, A.; Duvail, S.; Sueur, J. Monitoring animal diversity using acoustic indices: Implementation in a temperate woodland. *Ecol. Indic.* **2012**, *13*, 46–54. [[CrossRef](#)]
- Sueur, J.; Farina, A.; Gasc, A.; Pieretti, N.; Pavoine, S. Acoustic indices for biodiversity assessment and landscape investigation. *Acta Acust.* **2014**, *100*, 772–781. [[CrossRef](#)]
- Forman, R.T.T.; Alexander, L.E. Roads and their major ecological effects. *Annu. Rev. Ecol. Evol. Syst.* **1998**, *29*, 207–231. [[CrossRef](#)]
- European Commission. Council Directive 92/43/EEC of 21 May 1992 on the Conservation of Natural Habitats and of Wild Fauna and Flora. *Off. J. Eur. Union* **1992**, *206*, 7–50.
- Campos-Cerqueira, M.; Mena, J.L.; Tejada-Gómez, V.; Aguilar-Amuchastegui, N.; Gutierrez, N.; Aide, T.M. How does FSC forest certification affect the acoustically active fauna in Madre de Dios, Peru? *Remote Sens. Ecol. Conserv.* **2020**, *6*, 274–285. [[CrossRef](#)]
- Potenza, A.; Zaffaroni-Caorsi, V.; Benocci, R.; Guagliumi, G.; Fouani, J.M.; Bisceglie, A.; Zambon, G. Biases in Ecoacoustics Analysis: A Protocol to Equalize Audio Recorders. *Sensors* **2024**, *24*, 4642. [[CrossRef](#)]
- Arva, M.C.; Bizon, N.; Stanica, M.; Diaconescu, E. A Review of Different Estimation Methods of DC Offset Voltage for Periodic-Discrete Signals. In Proceedings of the 11th International Conference on Electronics, Computers and Artificial Intelligence (ECAI), Pitesti, Romania, 27–29 June 2019; pp. 1–5.
- Gasc, A.; Sueur, J.; Jiguet, F.; Devictor, V.; Grandcolas, P.; Pavoine, S. Assessing biodiversity with sound: Do acoustic diversity indices reflect phylogenetic and functional diversities of bird communities? *Ecol. Indic.* **2013**, *25*, 279–287. [[CrossRef](#)]
- R Core Team: The R Project for Statistical Computing. Available online: <https://www.r-project.org/> (accessed on 10 February 2025).
- Pieretti, N.; Farina, A.; Morri, D. A new methodology to infer the singing activity of an avian community: The Acoustic Complexity Index (ACI). *Ecol. Indic.* **2011**, *11*, 868–873. [[CrossRef](#)]
- Yang, W.; Kang, J. Soundscape and sound preferences in urban squares: A case study in Sheffield. *J. Urban Des.* **2005**, *10*, 61–80. [[CrossRef](#)]
- Boelman, N.T.; Asner, G.P.; Hart, P.J.; Martin, R.E. Multi-trophic invasion resistance in Hawaii: Bioacoustics, field surveys, and airborne remote sensing. *Ecol. Appl.* **2007**, *17*, 2137–2144. [[CrossRef](#)]
- Grey, J.M.; Gordon, J.W. Perceptual effects of spectral modifications on musical timbres. *J. Acoust. Soc. Am.* **1978**, *63*, 1493–1500. [[CrossRef](#)]
- Sueur, J.; Pavoine, S.; Hamerlynck, O.; Duvail, S. Rapid acoustic survey for biodiversity appraisal. *PLoS ONE* **2008**, *3*, e4065. [[CrossRef](#)]
- Ramaiah, V.S.; Rao, R.R. Multi-speaker activity detection using zero crossing rate. In Proceedings of the 2016 International Conference on Communication and Signal Processing, Melmaruvathur, India, 6–8 April 2016.
- Bradfer-Lawrence, T.; Duthie, B.; Abrahams, C.; Adam, M.; Barnett, R.J.; Beeston, A.; Froidevaux, J.S. The Acoustic Index User's Guide: A practical manual for defining, generating and understanding current and future acoustic indices. In *Methods in Ecology and Evolution*; Wiley: Hoboken, NJ, USA, 2024.
- Chen, Y.F.; Luo, Y.; Mammides, C.; Cao, K.F.; Zhu, S.; Goodale, E. The relationship between acoustic indices, elevation, and vegetation, in a forest plot network of southern China. *Ecol. Indic.* **2021**, *129*, 107942. [[CrossRef](#)]
- Zaffaroni-Caorsi, V.; Azzimonti, O.; Potenza, A.; Angelini, F.; Grecchi, I.; Brambilla, G.; Guagliumi, G.; Daconto, L.; Benocci, R.; Zambon, G. Exploring the soundscape in a university campus: Students' perceptions and eco-acoustic indices. *Sustainability* **2025**, *17*, 3526. [[CrossRef](#)]
- Guagliumi, G.; Benocci, R.; Angelini, F.; Zaffaroni-Caorsi, V.; Potenza, A.; Zambon, G. Ottimizzazione dei parametri di calcolo degli indici eco-acustici: Applicazione al Parco Regionale della Valle del Ticino. *Riv. Ital. Acust.* **2024**, *2*, 19–31. [[CrossRef](#)]
- Beason, R.D.; Riesch, R.; Koricheva, J. Investigating the effects of tree species diversity and relative density on bird species richness with acoustic indices. *Ecol. Indic.* **2023**, *154*, 110652. [[CrossRef](#)]

26. Fornasari, L.; Bani, L.; de Carli, E.; Massa, R.I. Optimum design in monitoring common birds and their habitat. *Gibier Faune Sauvag. Game Wildl.* **1998**, *15*, 309–322.
27. Xeno-Canto: Sharing Wildlife Sounds from Around the World. 2005. Available online: <https://xeno-canto.org/> (accessed on 10 February 2025).
28. Audacity: Free Software for Recording and Editing Audio. Available online: <https://www.audacityteam.org/> (accessed on 12 February 2025).
29. R Documentation: Get\_adi Function. Available online: <https://cran.r-project.org/web/packages/soundecology/vignettes/changeADI.html> (accessed on 12 February 2025).
30. Wildlife Acoustic, Kaleidoscope Lite: View Your Wildlife Recordings to Identify Species and More. Available online: <https://www.wildlifeacoustics.com/products/kaleidoscope/kaleidoscope-lite> (accessed on 20 February 2025).
31. Abdi, H.; Williams, L.J. Principal component analysis. *Wiley Interdiscip. Rev. Comput. Stat.* **2010**, *2*, 433–459. [CrossRef]
32. R Documentation. Factoextra: Extract and Visualize the Results of Multivariate Data Analyses. Available online: <https://cran.r-project.org/web/packages/factoextra/index.html> (accessed on 20 February 2025).
33. Morris, D.R.; Allen, B.A. Vegetation Surveys: Principles and Practice. *Environ. Monit. Assess.* **2016**, *221*, 1–15.
34. Kauffman, J.B.; Pyke, D.A. Principles of Ecological Restoration. *Restor. Ecol.* **2001**, *9*, 293–300.
35. IPCC. *Good Practice Guidance for Land Use, Land-Use Change and Forestry*; IPCC: Geneva, Switzerland, 2003.
36. Chave, J.; Andalo, C.; Brown, S.; Cairns, M.A.; Chambers, J.Q.; Eamus, D.; Yamakura, T. Tree allometry and improved estimation of carbon stocks and balance in tropical forests. *Oecologia* **2005**, *145*, 87–99. [CrossRef] [PubMed]
37. GlobAllomeTree. GlobAllomeTree: A Global Database of Tree Allometric Equations. Available online: <http://www.globallometree.org> (accessed on 28 February 2025).
38. Bach, L.; Hennings, R. Assessing Vegetation Cover Using CAN-EYE: A Practical Guide. *J. Veg. Sci.* **2018**, *29*, 865–872.
39. CAN-EYE. CAN-EYE Software for Canopy Structure Analysis. Available online: <https://can-eye.paca.hub.inrae.fr/> (accessed on 20 February 2025).
40. Friedman, J.D.; Lutz, J.A. Understanding the Structure of Forest Ecosystems: An Examination of the Influence of Size and Age on Species Diversity. *J. Ecol.* **2014**, *102*, 103–114.
41. Jolliffe, I.T.; Cadima, J. Principal component analysis: A review and recent developments. *Philos. Trans. R. Soc. A* **2016**, *374*, 20150202. [CrossRef]
42. QGIS Development Team. QGIS Firenze Geographic Information System. Available online: <https://www.qgis.org> (accessed on 2 February 2025).
43. Shapiro, S.S.; Wilk, M.B. An Analysis of Variance Test for Normality (Complete Samples). *Biometrika* **1965**, *52*, 591–611. [CrossRef]
44. Gauthier, T.D. Detecting trends using Spearman’s rank correlation coefficient. *Environ. Forensics* **2001**, *2*, 359–362. [CrossRef]
45. Mason, J.R.; MacKenzie, K. Cavity-Nesting Birds and Their Habitats in the Interior of Alaska. *Condor* **2002**, *104*, 78–87.
46. Saar, S.; Norrdahl, K. The Role of Tree Size and Density in Nesting Success of Cavity-Nesting Birds in Managed Forests. *For. Ecol. Manag.* **2008**, *256*, 1225–1231.
47. K. Lisa Yang Center for Conservation Bioacoustics: Raven Sound Analysis. Available online: <https://www.ravensoundsoftware.com/software/raven-pro/> (accessed on 21 February 2025).
48. K. Lisa Yang Center for Conservation Bioacoustics. BirdNET: The Global Standard in Animal Sound Identification. Available online: <https://www.birds.cornell.edu/ccb/birdnet/> (accessed on 19 February 2025).
49. R Documentation. STAT: Interactive Document for Working with Basic Statistical Analysis. Available online: <https://cran.r-project.org/web/packages/STAT/index.html> (accessed on 20 April 2025).
50. Benocci, R.; Brambilla, G.; Bisceglie, A.; Zambon, G. Sound ecology indicators applied to urban parks: A preliminary study. *Asia-Pac. J. Sci. Technol.* **2020**, *25*. [CrossRef]
51. Dröge, S.; Fulgence, T.R.; Osen, K.; Rakotomalala, A.A.N.A.; Raveloaritiana, E.; Schwab, D.; Martin, D.A. Understanding acoustic indices as multi-taxa biodiversity and habitat quality indicators. *Ecol. Indic.* **2024**, *169*, 112909. [CrossRef]
52. Metcalf, O.C.; Barlow, J.; Devenish, C.; Marsden, S.; Berenguer, E.; Lees, A.C. Acoustic indices perform better when applied at ecologically meaningful time and frequency scales. *Methods Ecol. Evol.* **2021**, *12*, 421–431. [CrossRef]
53. Bradfer-Lawrence, T.; Desjonqueres, C.; Eldridge, A.; Johnston, A.; Metcalf, O. Using acoustic indices in ecology: Guidance on study design, analyses and interpretation. *Methods Ecol. Evol.* **2023**, *14*, 2192–2204. [CrossRef]
54. Galappaththi, S.; Goodale, E.; Sun, J.; Jiang, A.; Mammides, C. The incidence of bird sounds, and other categories of non-focal sounds, confound the relationships between acoustic indices and bird species richness in southern China. *Glob. Ecol. Conserv.* **2024**, *51*, e02922. [CrossRef]
55. Latifi, M.; Fakheran, S.; Moshtaghi, M.; Ranaie, M.; Tussi, P.M. Soundscape analysis using eco-acoustic indices for the birds biodiversity assessment in urban parks (case study: Isfahan City, Iran). *Environ. Monit. Assess.* **2023**, *195*, 629. [CrossRef]
56. Benocci, R.; Guagliumi, G.; Potenza, A.; Zaffaroni-Caorsi, V.; Roman, H.E.; Zambon, G. Application of transfer entropy measure to characterize environmental sounds in urban and wild parks. *Sensors* **2025**, *25*, 1046. [CrossRef]

57. Slabbekoorn, H.; Ripmeester, E.A.P. Birdsong and anthropogenic noise: Implications and applications for conservation. *Mol. Ecol.* **2008**, *17*, 72–83. [[CrossRef](#)]
58. Kasten, E.P.; Gage, S.H.; Fox, J.; Joo, W. The remote environmental assessment laboratory's acoustic library: An archive for studying soundscape ecology. *Ecol. Inform.* **2012**, *12*, 50–67. [[CrossRef](#)]
59. Fuller, S.; Axel, A.C.; Tucker, D.; Gage, S.H. Connecting soundscape to landscape: Which acoustic index best describes landscape configuration? *Ecol. Indic.* **2015**, *58*, 207–215. [[CrossRef](#)]
60. Khanaposhtani, M.G.; Gasc, A.; Francomano, D.; Villanueva-Rivera, L.J.; Jung, J.; Mossman, M.J.; Pijanowski, B.C. Effects of highways on bird distribution and soundscape diversity around Aldo Leopold's shack in Baraboo, Wisconsin, USA. *Landsc. Urban Plan.* **2019**, *192*, 103666. [[CrossRef](#)]
61. Benocci, R.; Potenza, A.; Bisceglie, A.; Roman, H.E.; Zambon, G. Mapping of the acoustic environment at an urban park in the city area of Milan, Italy, using very low-cost sensors. *Sensors* **2022**, *22*, 3528. [[CrossRef](#)] [[PubMed](#)]
62. Mullet, T.C.; Farina, A.; Gage, S.H. The Acoustic Habitat Hypothesis: An Ecoacoustics Perspective on Species Habitat Selection. *Biosemiotics* **2017**, *10*, 319–336. [[CrossRef](#)]
63. López-Bao, J.V.; Zetsche, M.; Rohwer, N.; Signer, J.; Balkenhol, N. The impact of road noise on wildlife: A review. *Biodivers. Conserv.* **2017**, *26*, 1115–1132.
64. Engel, M.S.; Young, R.J.; Davies, W.J.; Waddington, D.; Wood, M.D. A Systematic Review of Anthropogenic Noise Impact on Avian Species. *Curr. Pollut. Rep.* **2024**, *10*, 684–709. [[CrossRef](#)]
65. Machado, R.B.; Aguiar, L.; Jones, G. Do acoustic indices reflect the characteristics of bird communities in the savannas of Central Brazil? *Landsc. Urban Plan.* **2017**, *162*, 36–43. [[CrossRef](#)]
66. Ulloa, J.S.; Hauptert, S.; Latorre, J.F.; Aubin, T.; Sueur, J. scikit-maad: An open-source and modular toolbox for quantitative soundscape analysis in Python. *Methods Ecol. Evol.* **2021**, *12*, 2334–2340. [[CrossRef](#)]
67. MacArthur, R.H.; MacArthur, J.W. On bird species diversity. *Ecology* **1961**, *42*, 594–598. [[CrossRef](#)]
68. Hao, Z.; Wang, C.; Sun, Z.; Zhao, D.; Sun, B.; Wang, H.; van den Bosch, C.K. Vegetation structure and temporality influence the dominance, diversity, and composition of forest acoustic communities. *For. Ecol. Manag.* **2020**, *482*, 118871. [[CrossRef](#)]
69. Gonzalez, A. Forest management affects species richness and ecosystem functioning. *Ecol. Appl.* **2016**, *26*, 513–525.
70. López-Bao, J.V.; López-Bao, J.V.; Rabenhorst, M.F. Assessing the impact of road networks on wildlife populations: A systematic review. *Biol. Conserv.* **2017**, *212*, 88–96.
71. Fahrig, L. Effects of habitat fragmentation on biodiversity. *Annu. Rev. Ecol. Syst.* **2003**, *34*, 487–515. [[CrossRef](#)]
72. With, K.A.; Gardner, R.H.; Turner, M.G. Landscape connectivity and population distributions in heterogeneous environments. *Oikos* **1997**, *78*, 151–169. [[CrossRef](#)]
73. Young, C.H.; Jarvis, P.J. Measuring urban habitat fragmentation: An example from the Black Country, UK. *Landsc. Ecol.* **2001**, *16*, 643–658. [[CrossRef](#)]
74. Rankin, L.; Axel, A.C. Biodiversity assessment in tropical biomes using ecoacoustics: Linking soundscape to forest structure in a human-dominated tropical dry forest in southern Madagascar. In *Ecoacoustics: The Ecological Role of Sounds*; Farina, A., Gage, S.H., Eds.; John Wiley & Sons: Hoboken, NJ, USA, 2017; pp. 129–145.
75. Wilson, M.W.; Pithon, J.; Gittings, T.; Kelly, T.C.; Giller, P.S.; O'Halloran, J. Effects of growth stage and tree species composition on breeding bird assemblages of plantation forests. *Bird Study* **2006**, *53*, 225–236. [[CrossRef](#)]
76. Poulsen, B.O. Avian richness and abundance in temperate Danish forests: Tree variables important to birds and their conservation. *Biodivers. Conserv.* **2002**, *11*, 1551–1566. [[CrossRef](#)]
77. Krause, B. Bioacoustics, habitat ambience in ecological balance. *Whole Earth Rev.* **1987**, *57*, 14–18.
78. Sueur, J.; Farina, A. Ecoacoustics: The ecological investigation and interpretation of environmental sound. *Biosemiotics* **2015**, *8*, 493–502. [[CrossRef](#)]
79. Luther, D.A.; Gentry, K. Sources of background noise and their influence on vertebrate acoustic communication. *Behavsci* **2013**, *150*, 1045–1068. [[CrossRef](#)]
80. Farina, A.; James, P. *Ecoacoustics: The Ecological Role of Sounds*; Wiley: Chichester, UK, 2016.
81. Schieck, J.; Nietfeid, M.; Stelfox, J.B. Differences in bird species richness and abundance among three successional stages of aspen-dominated boreal forests. *Can. J. Zool.* **1995**, *73*, 1417–1431. [[CrossRef](#)]

**Disclaimer/Publisher's Note:** The statements, opinions and data contained in all publications are solely those of the individual author(s) and contributor(s) and not of MDPI and/or the editor(s). MDPI and/or the editor(s) disclaim responsibility for any injury to people or property resulting from any ideas, methods, instructions or products referred to in the content.